

INVESTIGATION OF VORTEXING AND SWIRL
WITHIN A CONTAINMENT RECIRCULATION SUMP
USING A HYDRAULIC MODEL
SEABROOK NUCLEAR POWER STATION

by
Mahadevan Padmanabhan

Research Sponsored by
Yankee Atomic Electric Company

ARL ALDEN RESEARCH LABORATORY
WORCESTER POLYTECHNIC INSTITUTE

January 1980

25-81/M296HF

8112010642 811127
PDR ADOCK 05000443
A PDR

INVESTIGATION OF VORTEXING AND SWIRL WITHIN A
CONTAINMENT RECIRCULATION SUMP USING A HYDRAULIC MODEL

SEABROOK NUCLEAR POWER STATION

by

M. Padmanabhan

Research Sponsored by
Yankee Atomic Electric Company

George E. Hecker, Director

ALDEN RESEARCH LABORATORY
WORCESTER POLYTECHNIC INSTITUTE
HOLDEN, MASSACHUSETTS 01520

January 1980

ABSTRACT

Yankee Atomic Electric Company authorized the Alden Research Laboratory (ARL) of Worcester Polytechnic Institute (WPI) to conduct extensive hydraulic model testing of the Reactor Containment Sump of the Seabrook Nuclear Power Plant, Units 1 and 2.

The main purpose of the model study was to verify that the reactor containment sump would perform satisfactorily without the development of any severe vortices or other flow irregularities that could affect the operation of the pumps in the Emergency Core Cooling System (ECCS) during the recirculation mode.

A model was designed and constructed to a uniform scale of 1:4 to include the sump and surrounding area of the containment building with all the structures that could influence the approach flow. Tests based on Froude similarity incorporating various possible flow and pump combinations under different possible restrictions, such as screen blockage, were undertaken. Detailed studies on possible scale effects of modeling vortices were conducted before projecting model results to prototype performance. This involved higher temperature and higher velocity tests in the model than indicated by the Froude scaling criteria.

Results of the tests indicated no objectionable vortexing and swirl for all the possible operating conditions tested, and hence the original design of the sump was considered satisfactory. Evaluation of inlet loss coefficients under different flow conditions was also performed in order to verify the available net positive suction head ($NPSH_{AV}$) at the pumps.

TABLE OF CONTENTS

	<u>Page No.</u>
ABSTRACT	i
TABLE OF CONTENTS	ii
INTRODUCTION	1
PROTOTYPE DESCRIPTION	3
Reactor Building	3
The Containment Recirculation Sump	3
Operating Cases for Tests	4
ADVERSE FLOW CONDITIONS TO BE INVESTIGATED	5
SIMILITUDE	7
Froude Scaling	9
Similarity of Vortex Motion	10
Equal Velocity Rule	12
High Temperature-High Velocity Testing	12
MODEL DESCRIPTION AND INSTRUMENTATION	14
General Layout	14
Piping Details	14
Model Operation	15
Screens and Gratings	16
Observation Techniques	16
TEST PROCEDURE	16
Phase 1 - Test Series	17
Phase 2 - Test Series	17
Phase 3 - Test Series	18
RESULTS AND DISCUSSIONS	19
Phase 1 Tests	19
Phase 2 Tests	19
Phase 3 Tests	20
SUMMARY AND CONCLUSIONS	23
REFERENCES	25
TABLES	
PHOTOGRAPHS	
FIGURES	

INTRODUCTION

The reactor containment building of the Seabrook Nuclear Power Station, Unit 1, is provided with an emergency core cooling system (ECCS) designed to cool the shutdown reactor core and the containment in the event of a loss of coolant accident (LOCA). The ECCS injects water to maintain core cooling and initially the water for this is drawn from the refueling water storage tank (RWST). When the water level in this tank is depleted to a predetermined level, the ECCS is switched from injection to recirculation mode. At this point, water is drawn from the containment recirculation sump containing water drained from the break and the quench spray system. The approach flow to the sump is affected by the equipments and appurtenant structures forming obstructions to the flow. The water level, the discharges from the sump, and the water temperature could vary over a wide range during the recirculation mode, which lasts for an extended period of time to provide sufficient heat removal. It is very important that no adverse flow conditions that could affect performance of the pumps exist within the sump or the suction pipes. It is crucial that no air entraining vortices are formed and that the total intake losses are of a magnitude such that required NPSH of the pumps is satisfied.

The Alden Research Laboratory (ARL) was authorized by Yankee Atomic Electric Company (YAEC) to construct and test a model of the Seabrook Nuclear Power Station containment recirculation sump with the object of investigating any free surface vortex formation or other undesirable flow conditions that could adversely affect the performance of the various pumps of the Emergency Core Cooling Water System (ECCS) in the recirculation mode. Operating conditions involving a wide range of various possible approach flow distributions, water depths, water temperatures, screen blockage effects, and pump operating combinations were to be tested in the model. If potentially undesirable flow conditions occurred, modifications in the sump configuration were to be developed. Factors subject to careful investigation in the model study were air entrainment due to vortexing or other reasons, swirl in the suction pipes, and the inlet losses at the sump. Potential scale effects on vortices and similarity of screen influence on flow pattern were examined and extrapolated to the prototype towards establishing the conclusions of the study.

This report presents a description of the prototype and model, and summarizes similitude considerations, test procedures, instrumentation, conditions investigated, interpretation of results, and recommendations.

PROTOTYPE DESCRIPTION

Reactor Building

The reactor building is circular in plan, as shown in Figure 1, bounded by the containment wall, 4.5 ft thick with an inner radii of 70 ft. An inner wall of the same thickness encloses the steam generators, coolant pumps, filter units, and the connected accessories, as seen in Figure 1. The annular portion between the above two walls accommodates the accessories like accumulators, instrument racks, pressure relief tanks, elevators, and stairs.

The Containment Recirculation Sump

Containment Recirculation sumps are located next to each other close to the containment wall between the two accumulators and extend from bearing 240 to 300 degrees approximately, as marked in Figure 1. The total sump area is more or less rectangular in plan, about 37 ft long and 9.0 ft wide, with a 3 ft thick wall in the middle separating the area into two sumps. Each of the sumps is provided with two cages of stainless steel gratings and fine screens with a solid top cover as indicated in Figure 2. The water will enter the sumps through the six approach faces of these 2 ft 3 inch high cages. The sump floor itself is depressed below the containment building floor by about 8 ft. The sumps are also provided with a missile shield (a 2 inch plate) about 3 ft above the top covers and supported by hangers onto the top covers. The building floor at the sump is at EL -26 ft, the sump floor is at EL -34 ft, top cover plate at EL -23ft 9 inches, and the top of the missile shield is at EL -20 ft 7-1/4 inches. The sumps will be submerged under all operating conditions with the minimum water level about 3 inches above the solid cover during the recirculation mode.

The top cover is provided with air vent holes to release any trapped air, which may have accumulated as the water level increases. The average approach velocity upstream of the grating will be about 0.10 fps at the minimum submergence conditions without any screen and grating blockages.

The two horizontal outlet pipes are 16 inches in diameter (Sch. 40), and are provided with bellmouth entrances of 24 inches diameter. The center of the pipes at entrance is at EL -31 ft 6 inches, and the centerlines of the left and right pipes are at 7 ft and 4 ft away from the centerline of the dividing wall, respectively.

The water from the containment sprays and any potential pipe break would not directly impinge in the annular region containing the sump as the latter is separated by the inner wall. This water will enter the annular region through two rectangular openings in front of the sump and from the openings in the sides (in the regions of 200° and 340° bearing) far away from the sump. The two rectangular openings are provided with a deflector (Figure 1) to avoid water entering from these openings from flowing directly into the sump and also to prevent any breakflow jets being directed towards the sump.

Operating Cases for Tests

At the start of the recirculation mode of the ECCS (approximately 1800 seconds after LOCA), one Residual Heat Removal (RHR) and one Containment Spray (CS) pump begin to take suction from each containment sump. These are the only pumps which directly take suction from the containment sumps. Flow from each RHR pump goes to the inlet of either two safety injection or two charging pumps, and to the reactor coolant system through a parallel flow path. Flow from each CS pump returns to the containment environment via spray headers. Table 1 shows the ranges of flows possible depending upon the combinations of pumps taking suction from each sump, and these were used as operating cases for testing. As seen from the table, the maximum flow per suction pipe from the sump is limited to 7850 gpm. The minimum and maximum water levels were taken as EL -23 ft 6 inches and EL -20 ft 8 inches, respectively. The above flows and water levels were provided by United Engineers.

ADVERSE FLOW CONDITIONS TO BE INVESTIGATED

The following are some of the likely flow conditions in a containment recirculation sump which could cause poor pump performance and hence were investigated during the model study.

1. **Entrained Air** - Air entrainment in the suction pipes could be due to air entraining vortices existing in the sump, due to suction of entrapped air below top cover plates in a submerged sump, or due to any other specific reasons, such as breakflow jet impingement. It is established that even a low air concentration in the suction pipes, such as 3 to 5%, could lower the efficiency of the pump considerably (1). Hence, air entrainment is recognized as a major flow condition in the sump to be examined. Air entraining vortices (Types 5 or 6 of ARL Classification, Figure 3), are not acceptable. However, due to scale effects in a Froudian model, it is possible that a Type 3 or 4 vortex in the model could represent a Type 5 or 6 in the prototype. It is important to demonstrate that scale effects are negligible or to predict prototype performance using a suitable method. ARL uses a special high temperature-high flow test procedure to establish this aspect, apart from using the "Equal Velocity Rule" described in the subsequent sections.

The potential for air entrainment within the sump due to breakflow jet impingement is considered unlikely in this case as the sump is located outside the crane wall, far away from the break locations. Also, there will be a flow deflector wall in front of the opening in the crane wall near the sump.

2. **Swirling Flow** - The various possible approach flow patterns, together with possible vortexing, could induce considerable swirl in the suction pipes, and this would be undesirable for the pumps. Excessive swirl could cause unsteady loading on the impeller, and could also affect the intake losses and pipe friction losses, thereby affecting

the available NPSH for the pump. Measurement of swirls is accomplished in the model using a vortimeter in the suction pipe. It has not been well established what degree of swirl is allowable. Hence, to be conservative, it is desirable to eliminate or suppress the swirl to the extent possible.

3. Losses Leading to Insufficient NPSH - A poorly designed sump could result in large intake losses. Intake losses caused by screens, poor entrance conditions, vortex suppression devices, etc., may add up to a value such that the required NPSH of the pump is not satisfied. The water temperature could also affect the available NPSH due to vapor pressure variations. The inlet losses are difficult to be calculated theoretically and model tests give a much more reliable value of inlet losses. Separate tests were also conducted to establish the effect of swirl on friction losses in a pipe. With the derived values of the inlet and pipe losses, the NPSH available should be checked by recalculations.

The pipeline pressure gradient for a particular test was obtained by measuring the water columns connected to piezometric taps, and an average friction gradient line was obtained from this data. The determination of the loss coefficients was achieved using the common procedure (2) of extrapolating the measured pipeline gradient to the inlet and computing the head loss, h_L , as

$$h_L = \Delta h - u^2/2g \quad (1)$$

where Δh is the head loss between the containment water surface (at a point outside the sump) and the extrapolated pressure gradeline at the pipe inlet. The loss coefficient, C_L , was defined as:

$$C_L = \frac{h_L}{u^2/2g} \quad (2)$$

where $u^2/2g$ represents the velocity head in the pipe. Figure 4 shows a typical evaluation of C_L from pressure gradient data.

SIMILITUDE

The study of dynamically similar fluid motions forms the basis for the design of models and the interpretation of experimental data. The basic concept of dynamic similarity may be stated as the requirement that two systems with geometrically similar boundaries have geometrically similar flow patterns at corresponding instants of time (3). Thus, all individual forces acting on corresponding fluid elements of mass must have the same ratios in the two systems.

The condition required for complete similitude may be developed from Newton's second law of motion:

$$F_i = F_p + F_g + F_v + F_t \quad (3)$$

where

F_i = inertia force, defined as mass, M , times the acceleration, a

F_p = pressure force connected with or resulting from the motion

F_g = gravitational force

F_v = viscous force

F_t = force due to surface tension

Additional forces may be relevant under special circumstances, such as fluid compression, magnetic or Coriolis forces, but these had no influence on this study and were, therefore, not considered in the following development.

Equation (3) can be made dimensionless by dividing all the terms by F_i . Two systems which are geometrically similar are dynamically similar if both satisfy the dimensionless form of the equation of motion, Equation (3). We may write each of the forces on the right side of Equation (3) as:

$$F_p = \text{net pressure} \times \text{area} = \alpha_1 \Delta p L^2$$

$$F_g = \text{specific weight} \times \text{volume} = \alpha_2 \gamma L^3$$

$$F_v = \text{shear stress} \times \text{area} = \alpha_3' \mu \Delta u / \Delta y \times \text{area} = \alpha_3 \mu u L$$

$$F_t = \text{surface tension} \times \text{length} = \alpha_4 \sigma L$$

$$F_i = \text{density} \times \text{volume} \times \text{acceleration} = \alpha_5' \rho L^3 \times \text{acceleration} \\ = \alpha_5 \rho u^2 L^2$$

where

$\alpha_1, \alpha_2, \text{ etc.}$ = proportionality factors

L = representative linear dimension

Δp = net pressure

γ = specific weight

μ = dynamic viscosity

σ = surface tension

ρ = density

u = representative velocity

Substituting the above terms in Equation (3) and making it dimensionless by dividing the inertial force, we obtain

$$\frac{\alpha_1}{\alpha_5} E^{-2} + \frac{\alpha_2}{\alpha_5} F^{-2} + \frac{\alpha_3}{\alpha_5} R^{-1} + \frac{\alpha_4}{\alpha_5} W^{-2} = 1 \quad (4)$$

where

$$E = \frac{u}{\sqrt{\Delta p / \rho}} = \text{Euler number} \propto \frac{\text{Inertia Force}}{\text{Pressure Force}}$$

$$F = \frac{u}{\sqrt{gL}} = \text{Froude number} \propto \frac{\text{Inertia Force}}{\text{Pressure Force}}$$

$$R = \frac{u L}{\mu / \rho} = \text{Reynolds number} \propto \frac{\text{Inertia Force}}{\text{Viscous Force}}$$

$$W = \frac{u}{\sqrt{\sigma / \rho L}} = \text{Weber number} \propto \frac{\text{Inertia Force}}{\text{Surface Tension Force}}$$

Since the proportionality factors, α , are the same in model and prototype, complete dynamic similarity is achieved if all the dimensionless groups, E , F , R , and W , have the same values in model and prototype. In practice, this is difficult to achieve. For example, to have the values of F and R the same requires either a 1:1 "model" or a fluid of very low kinematic visco-

sity in the reduced scale model. Hence, the accepted approach is to select the predominant force and design the model according to the appropriate dimensionless group. The influence of other forces would be secondary and are called scale effects (2, 3).

Froude Scaling

Models involving a free surface are constructed and operated using Froude similarity since the flow process is controlled by gravity and inertia forces. The Froude number, representing the ratio of inertia to gravitational force,

$$F = u/\sqrt{gs} \quad (5)$$

where

- u = average velocity in the pipe
- g = gravitational acceleration
- s = submergence

was, therefore, made equal in model and prototype

$$F_r = F_m/F_p = 1 \quad (6)$$

where m, p, and r denote model, prototype, and ratio between model and prototype, respectively.

In modeling of an intake sump to study the formation of vortices, it is important to select a reasonably large geometric scale to achieve large Reynolds numbers and to reproduce the curved flow pattern in the vicinity of the intake (4). A geometric scale of $L_r = L_m/L_p = 1/4.0$ was chosen for the model, where L refers to length. At higher Reynolds number, an asymptotic behavior of energy loss coefficients with Reynolds number is usually observed in similar flows (2). Hence, with $F_r = 1$, the basic Froudeian scaling criterion, the Euler numbers, E, will be equal in model and prototype. This implies that the flow patterns and loss coefficients are equal in model and prototype. From Equation (6), using $s_r = L_r$, the velocity, discharge, and time scales were:

$$u_r = L_r^{0.5} \quad (7)$$

$$Q_r = L_r^2 \quad u_r = L_r^{2.5} \quad (8)$$

$$t_r = L_r^{0.5} \quad (9)$$

Similarity of Vortex Motion

The fluid motions involving vortex formation in the sumps of low head pump intakes have been studied by several investigators (1, 4, 5, 6). Anwar (4) has shown by principles of dimensional analysis that the dynamic similarity of fluid motion in an intake is governed by the dimensionless parameters given by:

$$\frac{4Q}{u_\theta d^2}, \frac{u}{\sqrt{2gs}}, \frac{Q}{v s}, \text{ and } \frac{d}{2s}$$

where

Q = discharge through the inlet

u_θ = tangential velocity at a radius equal to that of the outlet pipe

d = diameter of the outlet pipe

Surface tension effects were neglected in this analysis. The influence of viscous effects was defined by the parameter $Q/(v s)$, known as a radial Reynolds number, R_R .

For similarity between the dimensions of a vortex of types up to and including the narrow air-core type, it was shown that the influence of R_R becomes negligible if $Q/(v s)$ greater than 10^3 . As strong air-core type vortices, if present in the model, would have to be eliminated by modified sump design, the main concern for interpretation of prototype performance based on the model performance would be on the similarity of weaker vortices, such as surface dimples and dye-cores. For the prototype of the present study, the values

of R_R for the operating temperature ranges of 80°F to 190°F ranged from 1×10^5 to 13×10^5 . The value of R_R for the 1:4 model was always greater than 10^3 for water temperature of 40°F and above. Referring to Daggett and Keulegan (5), the viscous effects on vortexing phenomenon would be negligible if the Reynolds number, $R = ud/\nu$, is greater than 3.2×10^4 . For a 1:4 model, the minimum value of R in this study would be 0.48×10^5 . Thus, viscous forces might be expected to have only a secondary role in the present study. If so, dynamic similarity is obtained by equalizing the parameters $4Q/u_0 d^2$, $u/\sqrt{2gs}$, and $d/2s$ in model and prototype. A Froudian model would satisfy this condition, provided the curved approach flow pattern in the vicinity of the sump is properly simulated, which requires a large size model. A 1:4 model satisfied this requirement (4). However, potential scale effects due to viscous forces in the present model were investigated by special testing procedures (7), which will be referred to in this report as high temperature-high velocity tests and discussed subsequently.

Viscous and surface tension forces could influence the formation and strength of vortices (4, 5). The relative magnitude of these forces on the fluid inertia force is reflected in the Reynolds and Weber numbers, respectively, which are defined as:

$$R = u d/\nu \quad (10)$$

$$W = \frac{u^2 d}{\sigma/\rho} \quad (11)$$

It was important for this study to ascertain any deviations in similitude attributable to viscous and surface tension forces in the interpretation of model results to prototype conditions. Surface tension effects were considered negligible inasmuch as strong vortices were unacceptable, and the free surface was essentially flat for all final tests. Moreover, an investigation using liquids of the same viscosity but different surface tension coefficients ($\sigma = 4.9 \times 10^{-3}$ lb/ft to 1.6×10^{-3} lb/ft) showed practically no effect of surface tension forces on vortex flow (5). Also,

for higher Weber number, W greater than 120, the surface tension effects have been shown to be negligible (8). For the 1:4 model, the minimum value of W was 720. The vortex severity, S , is therefore mainly a function of the Froude number, but could also be influenced by the Reynolds number.

$$S = S (F, R) \quad (12)$$

The possible scale effect due to different Reynolds number in the model and prototype was ascertained before predicting vortex types for the prototype based on model observations. For this projection, technique, and for consistent observations, it is convenient to classify the free surface vortices from a swirl to an air core type vortex, as shown in Figure 3.

Equal Velocity Rule

To compensate for the excessive viscous energy dissipation and consequently less intense model vortex, various investigators have proposed increasing the model flow and, therefore, the velocity, keeping the submergence constant. Operating the model at the prototype inlet velocity (pipe velocity) is believed by some researchers to achieve the desired results (1). This is often referred to as Equal Velocity Rule, and is considered to give conservative predictions of prototype performance. The test procedure for the present study would incorporate testing at prototype velocities in the pipe, in accordance to this rule.

High Temperature-High Velocity Testing

Figure 5 illustrates the method used to investigate scale effects and predict vortex types in the prototype based on model results (7). The ordinate F_r is the ratio of model to prototype Froude number while the abscissa is the inlet pipe Reynolds number, R . Assume the model to operate at flow less than Froude scaling (F_r less than 1) at point a_1 . By increasing the discharge in the model while keeping the same submergence and temperature, F_r and R are increased cor-

responding to a point, a_N , where a vortex of type N was first observed. The model Reynolds number can also be changed by varying the kinematic viscosity with temperature changes, and similar tests performed by locate b_N , another point on the locus of type N vortices. Extrapolation of the line of constant vortex strength of type N can be made to a prototype Reynolds number at the proper Froude number ($F_r = 1$), point p_N . The locus could indicate any expedient measure of vortex severity. Any scale effects due to viscous forces would be evaluated and taken into account by such a projection procedure. The high temperature-high velocity tests could also be used in the similar fashion for projecting the inlet loss coefficients (from the pressure gradient measurements) and the swirl severities (from vortimeter readings) over a wide range of Reynolds and Froude numbers.

The inlet loss coefficient, C_L (alternately, the coefficient of discharge), may be affected by circulation (5) and hence by vortex severity. In the absence of circulation, this loss coefficient would not show any increase with R , whereas increasing circulation associated with vortices could affect this trend. Hence, measurements of pressure gradient in the pipe and evaluation of the loss coefficients could help judging any increased losses due to vortex severity.

The effect of circulation on the coefficient of discharge has been previously investigated (5). The angular momentum of the flow due to the swirl and vorticity is approximately conserved through the inlet since the tangential shear is small (6). The angular velocity of the transmitted swirl could be measured using a cross vane vortimeter. From the number of vortimeter rotations per unit of time, n , a representative measure of the tangential velocity, u_t , could be obtained as:

$$u_t = \pi n d \quad (13)$$

d being the pipe diameter. The values of u_t may be used to compare the vortex severity. An angle of indicated swirl may be defined (6) as:

$$\theta = \tan^{-1} u_t/u \quad (14)$$

The vortimeter readings and the indicated swirl angle would provide an indication of the total induced swirl in the pipe.

MODEL DESCRIPTION AND INSTRUMENTATION

General Layout

A physical model of the containment sump and a portion of the reactor building forming the approach to the sump were constructed to a geometric scale of approximately 1:4 on an elevated platform, as shown in Photograph 1. The portion of the containment building modeled is marked in Figure 1.

The model was operated based on Froude scaling. The model was essentially a wooden tank formed as a segment of a circle in plan with a radius of about 17.5 ft. The model walls were about 2 ft high from the model floor, which was elevated by about 7 ft from the laboratory building floor. All the appurtenant structures in the vicinity of the sump that could influence the approach flow were simulated up to the maximum water level. The model floor and walls were constructed of wood with necessary supports and bracings. The walls at the depressed sump portion and the sump floor itself were made of plexiglass to facilitate observation and photography. The top cover plates of the sump were also made of plexiglass. Photograph 2 shows the sump portion in the model.

Piping Details

Two 4 inch diameter (3.8 inch ID) horizontal pipes about 10 ft long formed the suction pipes (Figure 6). Both the pipes were provided with a plexiglass removable window for inserting a vortimeter and for observational purposes. An extra length of suction pipes beyond the scaled length (up to the control valve) was modeled to provide sufficient length for pressure gradient data. Figure 6 shows the pipe layout and the suction pipes identified in this report by the numbers indicated therein. The pipes were about 10 ft long outside the model boundary and were connected to 6 inch horizontal pipes using expansion pieces. The two 6 inch pipes were connected to a closed intermediate steel tank which in turn was connected to the 12 inch suction pipe of a 20 HP centrifugal pump. The 6 inch pipes were provided with calibrated orifice plates for flow measurement. The 12 inch delivery pipe of the 20 HP

main supply pump delivered the water back to the model forming a closed loop system, which enabled easy water level settings and also helped in maintaining water quality. For fitting and emptying the model tank at the beginning and end of testing and also for water level adjustments, a separate 4 inch diameter pipe loop with a small 5 HP pump was used. The water in the model tank could thus be taken in and out of the laboratory building sump. It was also possible to heat the water in the model tank by recirculating it through a 50 HP boiler using a separate 6 inch line and a 3 HP pump. The water in the laboratory sump was cleaned continuously using a sand filter to ensure good water quality. The pipes were provided with air bleeds at high points to remove air during filling of the model.

The straight horizontal portion past the model wall of each of the two suction pipes were provided with ten pressure taps, one pipe diameter apart; the first one being at 21 pipe diameters from the bellmouth entrance (Figure 7). These pressure taps were connected to a manometer board. Separate piezometer tubings connected to four different points (two in the depressed portion) on the model floor enabled the pressure gradient measurements to be related to the water level inside and outside of the sump gratings and fine screens. The water levels in the tubes were measured with a moving point gage with vernier (to 0.001 ft) and the water levels in the tubes of the manometer board were read using photographic techniques or direct scaling as necessary. Photograph 3 shows the pressure taps and the manometer board.

Model Operation

The model tank was filled to the desired level using the 4 inch pipe loop with clean water from the laboratory sump. The main pump was then started and the flow in each pipe could be adjusted with the valves in the 6 inch lines as well as the valve in the delivery line to a desired flow as indicated by pressure drop across orifice meter. The water level in the model could be adjusted, if required, by adding or taking out more water from the laboratory sump. The water in the model tank could be recirculated through the boiler if heating was necessary.

Screens and Gratings

The sump portion of the model was provided with a vertical plastic square mesh grating (0.5 inch mesh, 0.5 inch thick) through which the approach flow entered. As the prototype head loss through this grating was negligibly small (less than 0.01 inch), the grating was not modeled to scale, but a grating of approximately the same open area was used in the model. However, the framework supporting the grating was modeled to scale, being of larger dimensions.

The fine screen was modeled to scale the actual head losses. A 0.125 inch mesh, 0.023 inch wire, fine screen was used in the model, which gave approximately the same pressure loss coefficients over the screen Reynolds number range in the model as the corresponding values for the corresponding prototype ranges.

Observation Techniques

For the identification and classification of vortices, visual and photographic observations were made using dye traces, cotton balls, etc. The measurement of swirl in the pipe inlets was accomplished using a crossed vane vortimeter which could be fixed to pipe 1 or 2 (Photograph 4).

TEST PROCEDURE

Tests were conducted in three phases, as indicated below.

Phase 1 - Preliminary test series - testing of numerous combinations of pump operations, discharges, water levels, and farfield blockages at normal ambient laboratory temperature - selection of a few critical combinations - determination of inlet loss coefficients.

Phase 2 - Retesting critical combinations at Froude scaled and prototype pipe velocities with grating/screen blockage - vortimeter readings for critical combinations - appraisal of the sump performance based on vortex severity, swirl severity, and entrance losses - evolving a revised sump design as necessary.

Phase 3 - Retesting the selected revised sump configuration - detailed screen blockage tests - high temperature-high velocity tests - detailed inlet loss evaluation - drawing conclusions on revised sump performance and recommendations.

A more detailed description of each of the testing phases follows.

Phase 1 - Test Series

Table 1 shows the details of ten operating cases considered for the testing. Testing was conducted for both $F_r = 1$ and 2 (Froude scaled and prototype velocities). It may be appropriate to expect the worst conditions for vortexing when maximum flow occurs at the lowest submergence. Various approach flow distributions were possible due to farfield obstructions and the location of breaks as indicated in Table 2. For the operating cases 8, 9, and 10 (maximum discharges) at the minimum submergence depth, tests were conducted with various approach flow distributions in a sequence to identify any effects of these on swirl and vortexing. If there were any noticeable effects, a few critical approach flow distributions and operating flow combinations were selected for further tests. The inlet loss coefficients were evaluated for both the suction pipes with the water level corresponding to the minimum water level with no blockage effects.

Phase 2 - Test Series

With the critical farfield approach flow distributions derived from Phase 1 testing, tests to identify vortex severities due to screen blockage were first undertaken. Twelve possible blockage schemes were tested with minimum water level and for operating Cases 8, 9, and 10 with 50% of the grating area blocked (Figure 8). Blockages were produced with aluminum strips placed on the grating. For each of the tests, extensive observations of vortexing, vortimeter readings, and flow patterns inside the sump were conducted. From these results, three worst blockage schemes were chosen to be tested for all the other operating cases not tested so far and for further tests such as inlet loss determination and high temperature-high velocity tests.

The results of Phase 1 and 2 tests were used to decide whether any changes in the design or location of the sump were necessary. If so, suitable modifications or a revised sump design were derived by further tests of cases where the problems were encountered. Phase 3 test series were to be conducted on the revised sump design, if found necessary.

Phase 3 - Test Series

These tests constituted the final series of tests on the selected sump design to confirm satisfactory performance of the sump. Extensive tests with selected blockage schemes were conducted for all the operating cases at both maximum and minimum water levels to identify any problems. Swirl measurements and vortex observations were made for this purpose for each run. The Froude number ratio was varied from 0.5 to 2.0 to obtain the inlet loss coefficients over a wide range of Reynolds numbers keeping the submergence constant and with a selected 50% screen blockage for one and two train operations. Additional tests to observe air entrapment beneath top covers and subsequent withdrawal were also conducted. The necessity of any more design changes were ascertained and effected if found needed.

The last part of Phase 3 tests were the high temperature-high velocity tests (explained earlier in the section on Similitude). The water was heated to temperatures from 50°F to 155°F. For four different temperatures in this range, the Froude number ratio was varied from 0.6 to 2.2 by changing flow, keeping submergence and screen blockage scheme to that of the worst operating case found from Phase 2 tests. Vortex severities and swirl indicated by vortimeter were observed for each flow setting. For a few test runs, pressure gradient measurements were also taken. All these results were used to identify scale effects if any.

RESULTS AND DISCUSSIONS

Phase 1 Tests

Phase 1 tests showed that for the operating cases considered, the farfield obstructions influenced to a small extent the approach flow pattern and hence the positions of the eddies and surface dimples observed within the sump. No significant influence of these approach flow patterns on the severity of vortices or intensities of swirl were observed. Only unstable and intermittent surface dimples and eddies were present inside the sump area. The maximum intensity of swirl corresponded to an indicated swirl angle of about 2 degrees for operating Case 8 at the minimum water level.

As a part of a preliminary testing, the inlet loss coefficient for pipe 1 over a Reynolds number range of 1.0 to 2.6×10^5 was evaluated for operating Cases 8 and 9 at the minimum water level and was found to be about 0.34 on the average with no screen or grating blockages.

Phase 2 Tests

A. Screen Blockage Tests

Various screen blockage schemes, producing up to 50% blockage as shown in Figure 8, were tested for operating cases 8 and 10 at both Froude scaled and prototype velocities to identify a few schemes producing severe vortexing and/or swirl. Table 3 gives the results of tests with prototype velocities ($F_r = 2$) for operating Case 8. As seen from Table 3, blockage schemes 2, 11, and 12 produced more intense vortexing or swirl compared to other schemes. Photographs 5a and 5b show the vortex activity for blockage scheme 12 and operating case 8 at scaled velocities and at prototype velocities in suction pipes, respectively, ($F_r = 1.0$ and 2.0). The vortices were unstable, intermittent, and occasionally stronger, and derived their energy mainly from eddies shed by the corners, columns, etc. Figures 9a and 9b illustrate the strongest vortex activities observed at $F_r = 2.0$ for operating case 8. Figure 9a shows the vortex

activity at maximum water level with blockage scheme 11, whereas Figure 9b shows the vortex activity at minimum water level with blockage scheme 12. As shown in these figures, the vortices were mostly of Types 2 and 3 (ARL classification, Figure 3) for $F_r = 2.0$. They were less intense, types 1 to 2, at Froude velocities, $F_r = 1$. The maximum indicated angle of swirl corresponded to screen blockage scheme 12 at minimum water level and was about 5 degrees for operating case 8. For operating case 10, no significant vortexing and swirl were observed.

B. Evaluation of Sump Performance

Phase 1 and 2 tests indicated neither air-entraining vortices nor any vortices with strong and coherent dye cores. The indicated swirl angles as noted from vortimeter readings were as small as 5 degrees, small enough to have practically no effects on entrance losses (confirmed by Phase 3 tests later) and only small effects on frictional losses as confirmed by separate tests (10). Hence, the sump was considered to perform satisfactorily and no need for modifications were indicated by Phase 1 and 2 tests.

Phase 3 Tests

A. Vortexing and Swirl

Extended tests were conducted to identify vortexing and swirl for all the ten operating cases with maximum and minimum water levels and with screen blockage schemes 2, 11, and 12 for both scaled and prototype velocities in the suction pipes. Photograph 6 shows the vortex activity for operating case 8 at maximum water level. Table 4 gives the results for tests with prototype velocities and as shown in this table no air entraining vortices were encountered for any of these cases. Only surface swirls, dimples, and eddies shed by corners were observed in most of the cases. The indicated swirl angles were in the range of 0-5 degrees.

B. High Temperature-High Velocity Tests

To establish whether any scale effects due to viscous forces exist and to predict the likely performance of the prototype based on vortexing and swirl, high temperature-high velocity tests, as described earlier in this report, were

undertaken. The model was run at operating case 8 with submergence corresponding to the minimum water level. Operating case 8 with 50% screen blockages as per schemes 11 and 12 was considered. The Froude number was varied by varying the flow through both suction pipes by equal proportions to give values of Froude number ratio, F_r , equal to 0.6, 1.0, 1.4, 1.8, and 2.2 for each of the four temperatures tested; namely, 56, 82, 121, and 155°F. Table 5 gives the results of these tests. Figure 10 shows the vortex types observed during the high temperature-high velocity tests for screen blockage scheme 12, which gave strongest vortex activity. Figure 11 shows the vortimeter readings for screen blockage scheme 11, which gave highest swirl levels. It could be seen that no observable changes in the vortex activity with Reynolds number existed for the same Froude number ratio (Figure 10). The locus of the vortices of a given severity was more or less horizontal, indicating no scale effects due to viscous effects. A prediction of vortex types in the prototype operating range under the same conditions would indicate only surface swirls and dimples and no vortices with any coherent cores.

Figure 11 shows the vortimeter readings and it can be seen that swirl intensities were also free from any scale effects. In short, Figures 10 and 11 confirmed that practically no scale effects due to viscous forces were apparent.

C. Inlet Loss Coefficients

Pressure gradient data were obtained for one pump and two pump operating cases over a range of Reynolds number from 1.0 to 6×10^5 . The data obtained for pipe 1 and for pipe 2 showed practically no significant differences in the value of C_L . Photograph 7 shows a typical hydraulic gradeline for pipe 1 obtained for operating case 8 with 50% screen blockage corresponding to scheme 12. Figures 12 and 13 show the C_L versus R data for pipes 1 and 2 for one and two pipe operations. No Reynolds number effect on values of C_L was observed. With an extension ring at the face of the bellmouth entrance (Figure 14), the pressure gradient measurements were repeated to see whether any reduction in C_L was possible and the results are included in Figures 12 and 13. The average value of C_L with 50% screen blockage was about 0.37 for one pipe operation and 0.33 for two pipe operation and showed practically no change

with the modified entrance. Hence, no modifications in the entrance design are recommended. Tables 6 and 7 show the complete results for original and modified entrances, respectively. The value of C_L indicates the total losses including the screen, grating, and entrance losses. The loss of head across the grating and screen was evaluated by separate tests and was found to be about 11.5 times the approach velocity head upstream of the grating.

D. Air Venting Under Cover Plates

During Phase 2 tests, it was noticed that considerable quantities of air were caught underneath the top cover while the sump was filled up. A venting system consisting of 1/8 inch diameter holes at 3 inch c/c on the top covers was found to be effective in the model. Hence, a similar system with at least three rows of 1/2 inch holes at 12 inch c/c for all top cover plates in the prototype is recommended.

E. Intensity of Swirl in Suction Pipes

Although neither air-entraining nor strong vortices with coherent cores were observed in the sump for any of the operating conditions, even with partial screen blockages for certain blockage schemes, swirling flow in the suction pipes with indicated swirl angles of up to 5 degrees was observed. The effect of the swirl on the entrance losses was included in the determined values of C_L explained in section (C) above. However, any possible effects of the swirl on the friction losses in the pipe was not known. Hence, a separate study was conducted to quantify this effect, and details of this are included in a separate ARL report (10). It was found that swirling flow with a 5 degree indicated swirl angle would increase the friction losses in the pipe up to about 9 percent. The NPSH calculations should take into account this increased friction loss. The swirl per se' is so small that its effects on the pump performance may be negligible.

SUMMARY AND CONCLUSIONS

A 1:4 undistorted scale model of the Containment Recirculation Sump of the Seabrook Nuclear Power Station was tested to ensure that undesirable flow patterns that could result in a poor performance of the pumps in the Emergency Core Cooling System will not exist for the various operating conditions during the recirculation mode. Extensive studies involving many possible combinations of pump operating cases, water surface elevations, and discharges were undertaken. These studies showed a satisfactory performance of the sump under all operating conditions tested, including partial blockage of the gratings and screens. Hence, no modifications in the sump design were found necessary. The negligible influence of possible scale effects in the Froude scaled model was ascertained using the results of high temperature-high velocity tests.

The essential findings of this hydraulic model study are itemized as follows:

1. As far as vortexing and swirl were concerned, the proposed Seabrook Containment sump was found to perform satisfactorily for all operating cases considered, including the asymmetrical blockage (up to 50%) of screens and gratings.
2. The maximum indicated swirl angle of the flow in the suction pipes was about 5 degrees. This swirl intensity may be too small to have any adverse affects on the pump performance. An increase in friction loss of up to about 9 percent is probable due to this swirling flow, as indicated by separate studies conducted at ARL (10).
3. A projection to the prototype performance, based on the results of the high temperature-high velocity tests showed that no objectionable vortexing problems would exist in the prototype. Only surface swirls, dimples, and surface eddies are expected in the sump area.

4. The inlet loss coefficients, C_L , for both the suction pipes were evaluated for a range of pipe Reynolds numbers, R . It was observed that no significant changes of C_L occurred within the wide range of R tested. The average values of the C_L for both the pipe inlets were about 0.37 with 50% screen blockage. This value of C_L includes losses due to screens and gratings.

5. Some air entrapment underneath the originally proposed solid top covers was observed in the model. As entrapped air is undesirable, it is recommended that each of the top covers be provided with at least three rows of 1/2 inch diameter holes at about 12 inches c/c. This will allow the air to escape as the water level rises in the sump.

REFERENCES

1. Denny, D.F., and Young, G.A.J., "The Prevention of Vortices and Swirl at Intakes," 7th General Meeting Transactions, IAHR, Lisbon, 1957.
2. Daily, J.W., and Harleman, D.R.F., Fluid Dynamics, Addison-Wesley Publishing Company, 1965.
3. Rouse, H., Handbook of Hydraulics, John Wiley & Sons, 1950.
4. Anwar, H.O., "Prevention of Vortices at Intakes," Water Power, p. 393, October 1968.
5. Daggett, L.L., and Keulegan, G.H., "Similitude Conditions in Free Surface Vortex Formations," Journal of Hydraulics Division, ASCE, Vol. 100, pp. 1565-1581, November 1974.
6. Reddy, Y.R., and Pickford, J., "Vortex Suppression in Stilling Pond Overflow," Journal of Hydraulics Division, ASCE, pp. 1685-1697, November 1974.
7. Durgin, W.W., and Hecker, G.E., "The Modeling of Vortices at Intake Structures," Joint Symposium on Design and Operation of Fluid Machinery, IAHR/ASME/ASCE, Colorado State University, June 1978.
8. Jain, A.K., Raju, K.G.R., and Garde, R.J., "Vortex Formation at Vertical Pipe Intakes," Journal of Hydraulics Division, ASCE, October 1978, p. 1429-1445.
9. Padmanabhan, M., and Vigander, S., "Pressure Drop Due to Flow Through Fine Mesh Screens," Journal of Hydraulics Division, ASCE, August 1978.
10. Janik, C.R., and Padmanabhan, M., "Effect of Swirling Flow on Friction Losses and Orifice Meter Calibration," ARL Report No.

TABLES

TABLE 1
Operating Cases

Operating Case No.	Discharge (gpm)	
	Sump 1	Sump 2
1	4100	3000
2	3000	4100
3	7400	3300
4	3300	7400
5	7850	3300
6	3300	7850
7	7400	7400
8	7800	7800
9	7850	0
10	0	7850

NOTE:

Minimum Water Level = EL -23'-6"

Maximum Water Level = EL -20'-8"

Containment Building
Floor Level = EL -26'-0"

Sump Bottom Floor
Level = EL -34'-0"

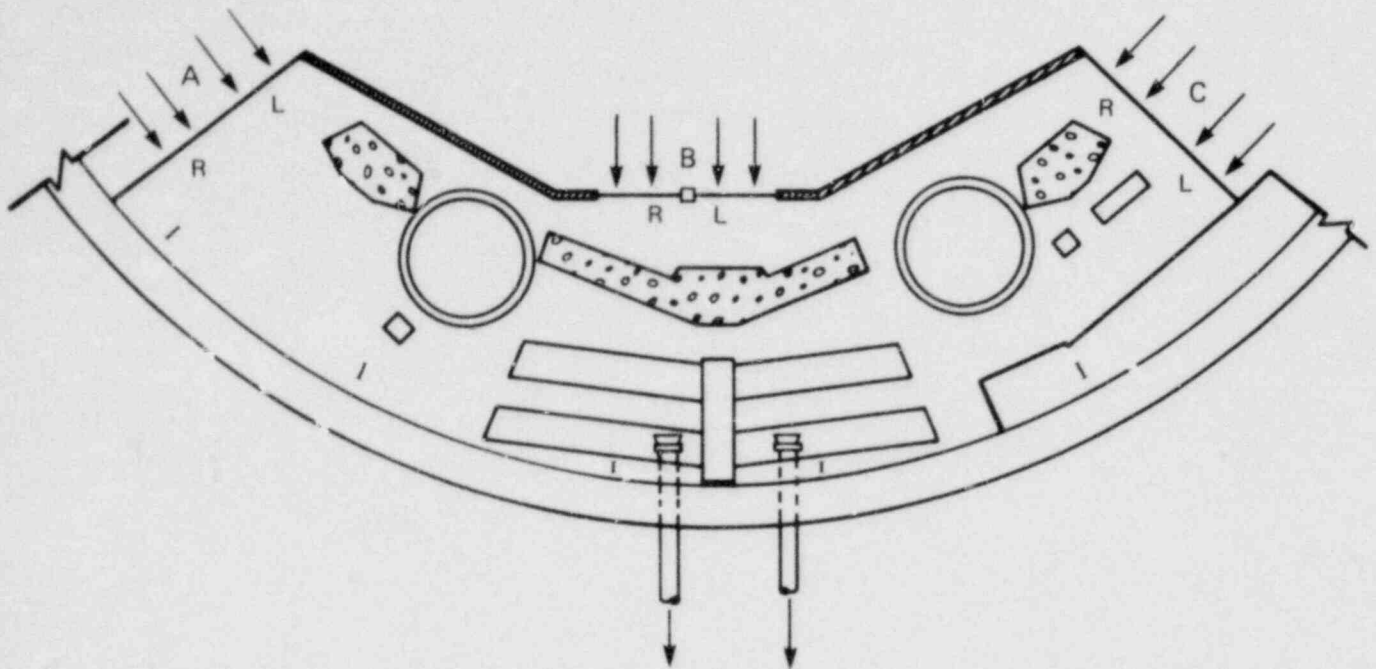
Pipe Centerline
Level = EL -31'-6"

Top Cover Elevation = EL -23'-9"

Range of water levels were assumed the same for all cases.

TABLE 2

Farfield Flow Distributions Tested



Distribution No.	Percent Open					
	A		B		C	
	L	R	L	R	L	R
1	100	100	0	0	100	100
2	100	100	100	0	100	100
3	100	100	0	0	100	0
4	100	100	0	100	100	100
5	100	100	100	0	100	0
6	100	100	0	100	100	0
7	100	100	0	0	0	100
8	100	100	100	100	100	0
9	100	100	100	100	0	100
10	100	0	0	0	100	100
11	100	0	100	0	100	100
12	100	0	0	100	100	100
13	100	0	0	0	100	100
14	C	100	100	100	100	100
15	100	0	100	100	100	100

TABLE 3

Vortex Observations for Various Blockage Schemes
 Tests with Prototype Velocities ($F_r = 2$) for Operating Case 8

<u>Test No.</u>	<u>Blockage Scheme</u>	<u>Vortex Types</u>	<u>Remarks</u>
1	1	0-1	
2	2	1-3	No stable core, vortimeter reading: 5 rev/100 sec
3	3	0-1	
4	4	0-1	
5	5	0-1	
6	6	0-1	Highly unstable swirl
7	7	0-1	
8	8	0-1	
9	9	0-1	
10	10	0-2	Very rare occurrence of dimple
11	11	0-1	Vortimeter readings high 55 rev/100 sec
12	12	1-3	No stable core, vortimeter readings: 5 rev/100 sec

TABLE 4

Vortexing and Swirl Observations for
Various Operating Cases with 50% Screen Blockage

<u>Operating Case No.</u>	<u>Water Surface Elevation (ft)</u>	<u>Blockage Scheme</u>	<u>F r</u>	<u>Vortex Types*</u>	<u>Vortimeter Reading Revs/100 sec</u>
1	-23'-6"	2	2.0	0-1	3
1	-23'-6"	11	2.0	0-1	12
1	-23'-6"	12	2.0	0-1	0
2	-23'-6"	2	2.0	0-1	0
2	-23'-6"	11	2.0	0-1	24
2	-23'-6"	12	2.0	0-1	0
3	-23'-6"	2	2.0	0-1	--
3	-23'-6"	11	2.0	0-1	14
3	-23'-6"	12	2.0	0-1	--
4	-23'-6"	2	2.0	1-2	--
4	-23'-6"	11	2.0	1-2	16
4	-23'-6"	12	2.0	1-2	--
5	-23'-6"	2	2.0	0-1	--
5	-23'-6"	11	2.0	0-1	16
5	-23'-6"	12	2.0	1-2	9
6	-23'-6"	2	2.0	0-1	--
6	-23'-6"	11	2.0	0-1	41
6	-23'-6"	12	2.0	0-1	0
7	-23'-6"	2	2.0	0-1	--
7	-23'-6"	11	2.0	0-1	53
7	-23'-6"	12	2.0	0-1	--
8	-23'-6"	2	2.0	0-1	--
8	-23'-6"	11	2.0	1-2	55
8	-23'-6"	12	2.0	1-3	5
8	-20'-4"	2	2.0	1-3	21
8	-20'-4"	11	2.0	1-2	12
8	-20'-4"	12	2.0	0-1	12
10	-23'-6"	2	2.0	1-2	10
10	-23'-6"	11	2.0	1-2	15
10	-23'-6"	12	2.0	1-2	1
10	-20'-4"	2	2.0	1-2	18
10	-20'-4"	11	2.0	1-2	29
10	-20'-4"	12	2.0	1-2	3

*Vortex activity was unstable and intermittent. Ranges of observed vortex types are indicated.

TABLE 5a
High Temperature-High Velocity Tests
Screen Blockage Scheme 11

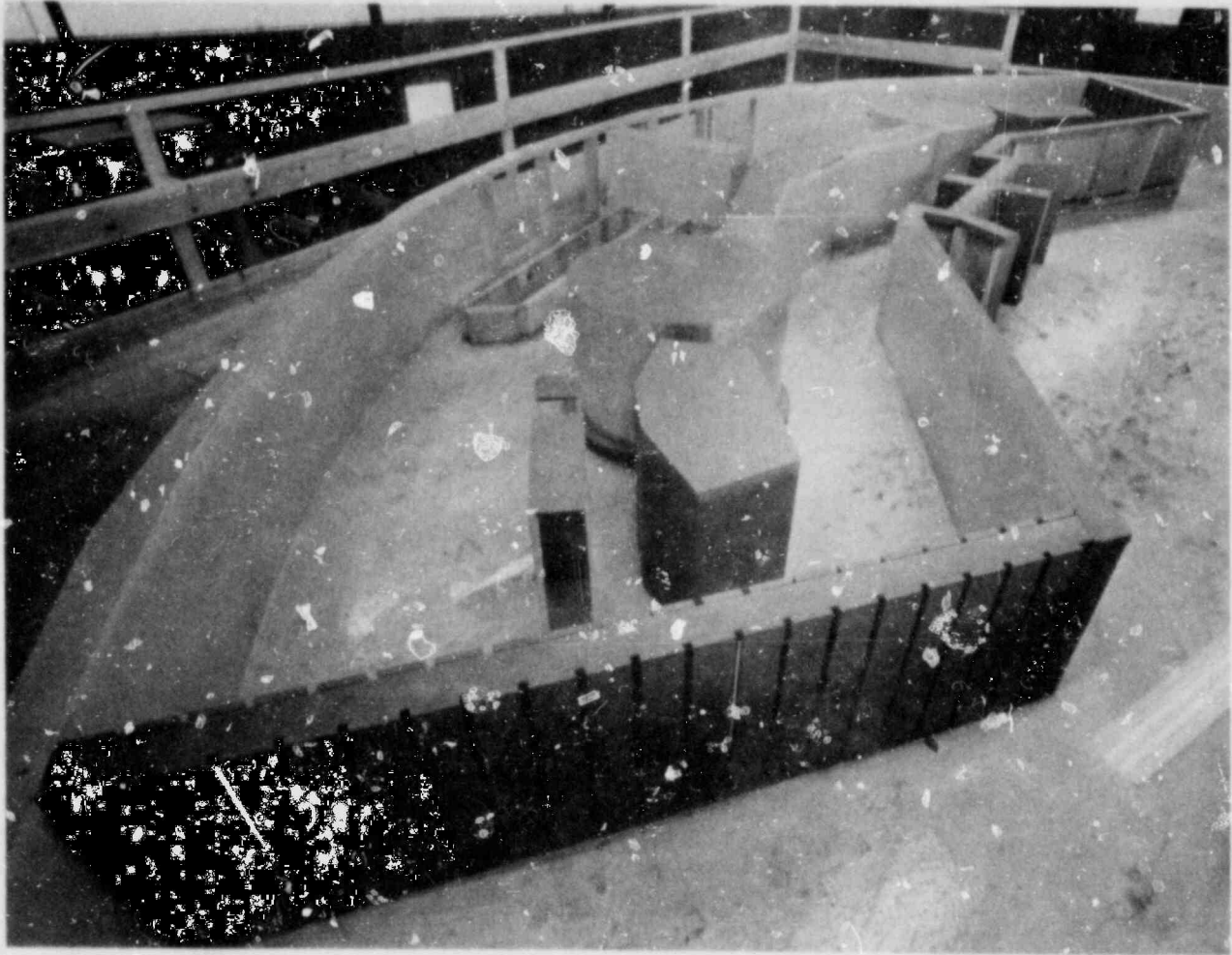
Test No.	Corresponding Prototype Discharge Per pipe, gpm	Froude Number Ratio $F_r = F_m/F_p$	Water Temp. °F	Model Reynolds Number $R = ud/\nu$ $R \times 10^{-5}$	Vortimeter Readings Rev./min	Vortex Types Observed	Remarks
T-2	17160	2.2	56	3.42	60 CW	0	No activity
T-3	14040	1.8	56	2.80	44 CW	0	No activity
T-6	10920	1.4	56	2.17	31 CW	1	Very slight surface swirl
T-7	7800	1.0	56	1.55	18 CW	0	No activity
T-10	4680	0.6	56	0.97	0 CW	0	No activity
T-12	17160	2.2	82	4.83	59 CW	1-2	Very intermittent and weak
T-13	14040	1.8	82	3.96	47 CW	1-2	Very intermittent and weak
T-16	10920	1.4	82	3.07	29 CW	0	No activity
T-17	7800	1.0	82	2.20	21 CW	0	No activity
T-20	4680	0.6	82	1.32	10 CW	0	No activity
T-21	17160	2.2	121	7.27	51 CW	1-2	Very intermittent and weak
T-24	14040	1.8	121	5.95	44 CW	1-2	Very intermittent and weak
T-25	10920	1.4	121	4.63	27 CW	1-2	Very intermittent and weak
T-28	7800	1.0	121	3.30	18 CW	0	No activity
T-29	4680	0.6	121	1.98	7 CW	0	No activity
T-32	17160	2.2	155	9.54	51 CW	1-2	Very intermittent and weak
T-33	14040	1.8	155	7.81	48 CW	1	Very intermittent and weak
T-36	10920	1.4	155	6.07	33 CW	1	Very intermittent and weak
T-37	7800	1.0	155	4.34	21 CW	0	No activity
T-40	4680	0.6	155	2.61	3 CW	0	No activity

TABLE 5b

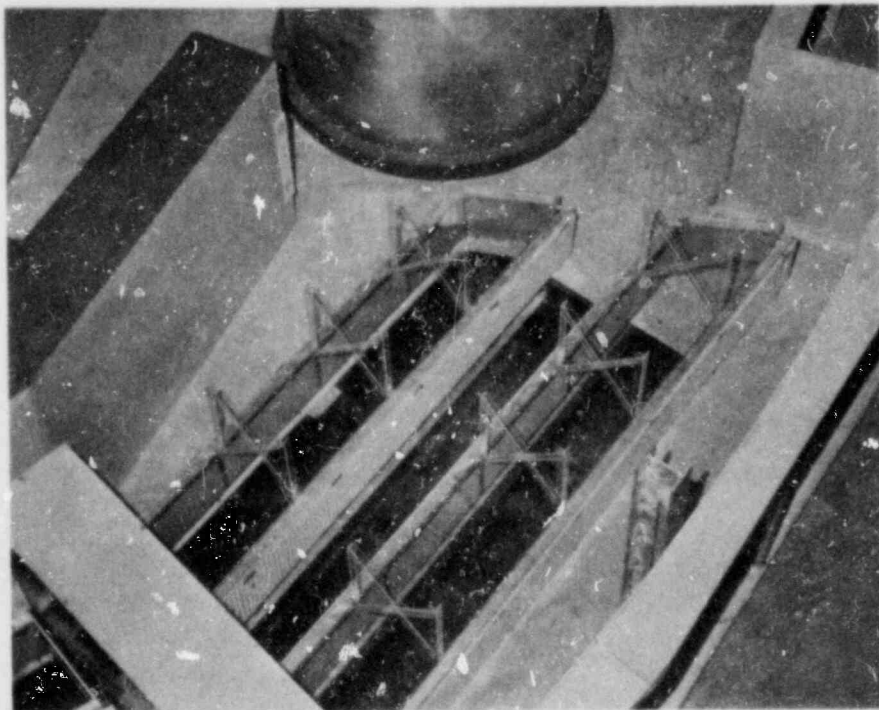
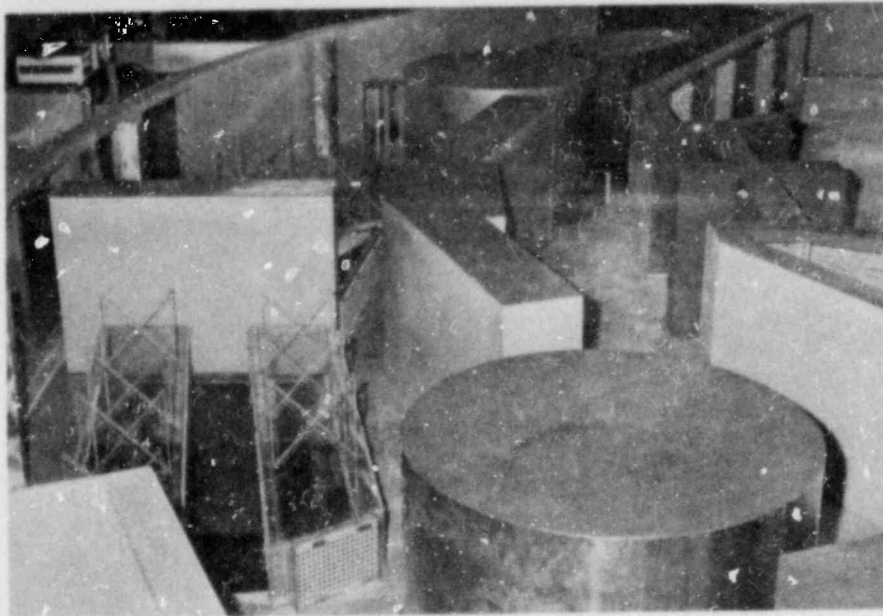
High Temperature-High Velocity Tests
Screen Blockage Scheme 12

Test No.	Corresponding Prototype Discharge Per pipe, gpm	Froude Number Ratio $F_r = F_m/F_p$	Water Temp. °F	Model Reynolds Number $R = ud/\nu$ $R \times 10^{-5}$	Vortimeter Readings Rev./min	Vortex Types Observed	Remarks
T-1	17160	2.2	56	3.42	1	1-3	Very slight surface swirl
T-4	14040	1.8	56	2.80	8	1-2	Very slight surface swirl
T-5	10920	1.4	56	2.17	2	1-2	Very slight surface swirl
T-8	7800	1.0	56	1.55	2	1	Eddies shed by objects
T-9	4680	0.6	56	0.93	0	0-1	No activity
T-11	17160	2.2	82	4.83	3	1-3	Very intermittent and weak
T-14	14040	1.8	82	3.96	4	1-2	Surface activity only
T-15	10920	1.4	82	3.07	0	0-1	No activity
T-18	7800	1.0	82	2.20	0	0-1	No activity
T-19	4680	0.6	82	1.32	1	0-1	No activity
T-22	17160	2.2	121	7.27	2	1-3	
T-23	14040	1.8	121	5.95	7	1-2	Swirls
T-26	10920	1.4	121	4.63	1	1-2	Eddies shed by objects
T-27	7800	1.0	121	3.30	1	0-1	No activity
T-30	4680	0.6	121	1.98	0	0-1	No activity
T-31	17160	2.2	155	9.54	7	1-3	Surface activity only
T-34	14040	1.8	155	7.81	18	1-2	
T-35	10920	1.4	155	6.07	14	1-2	
T-38	7800	1.0	155	4.34	2	0-1	No activity
T-39	4680	0.6	155	2.61	3	0-1	No activity

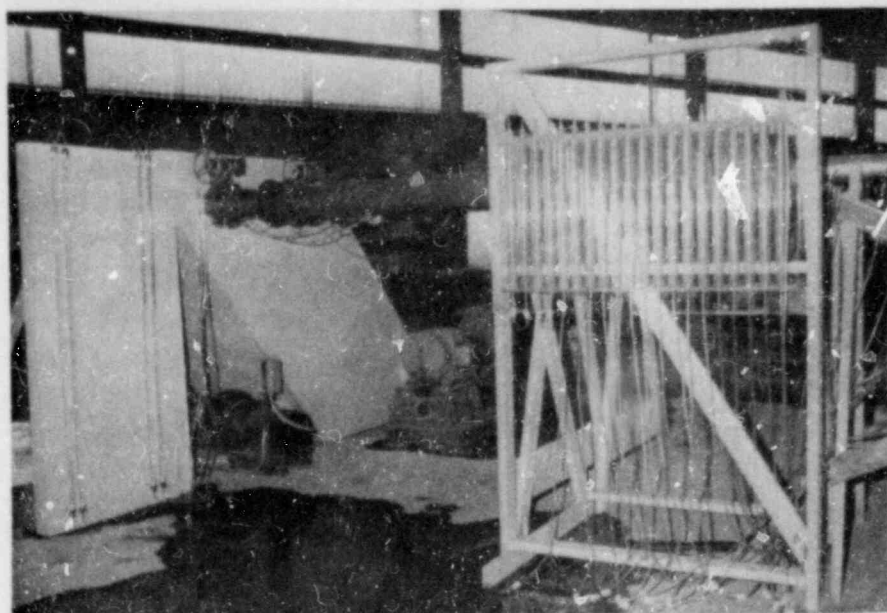
PHOTOGRAPHS



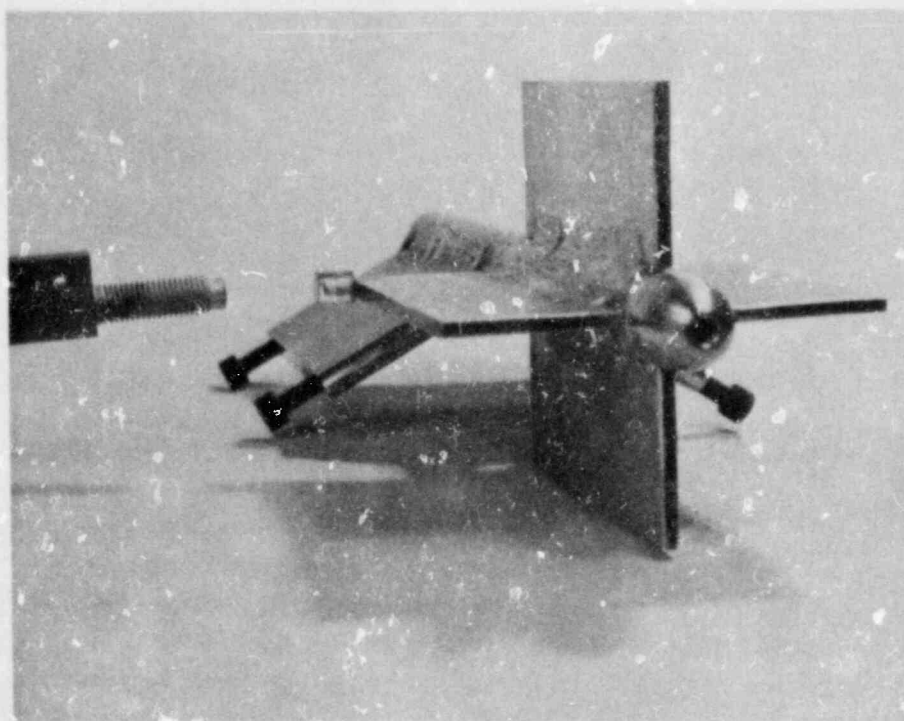
Photograph 1 1:4 Scale Containment Sump Model



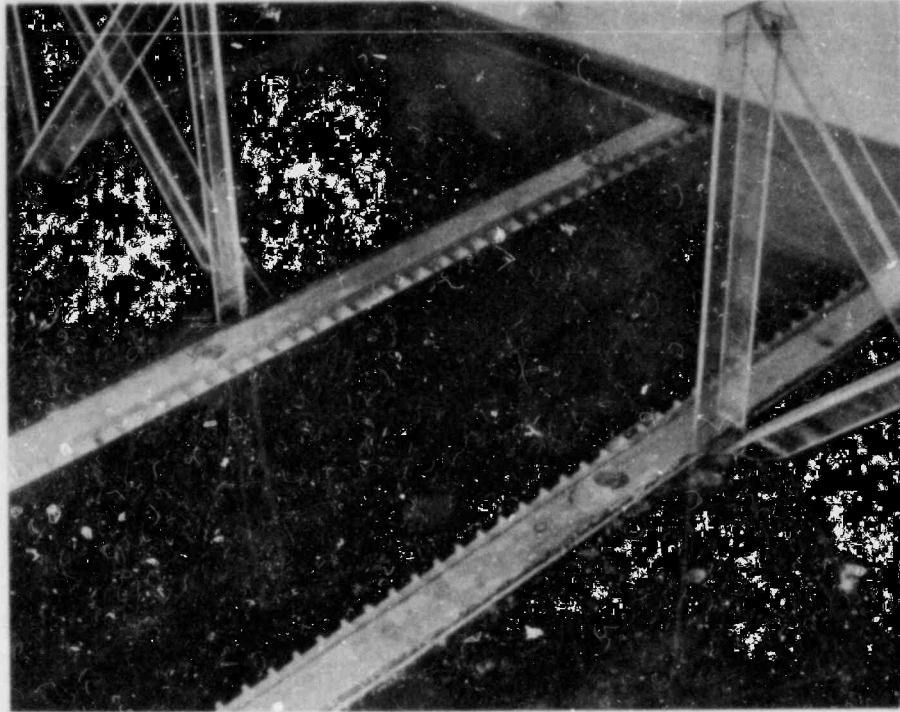
Photograph 2 Model Sump Details



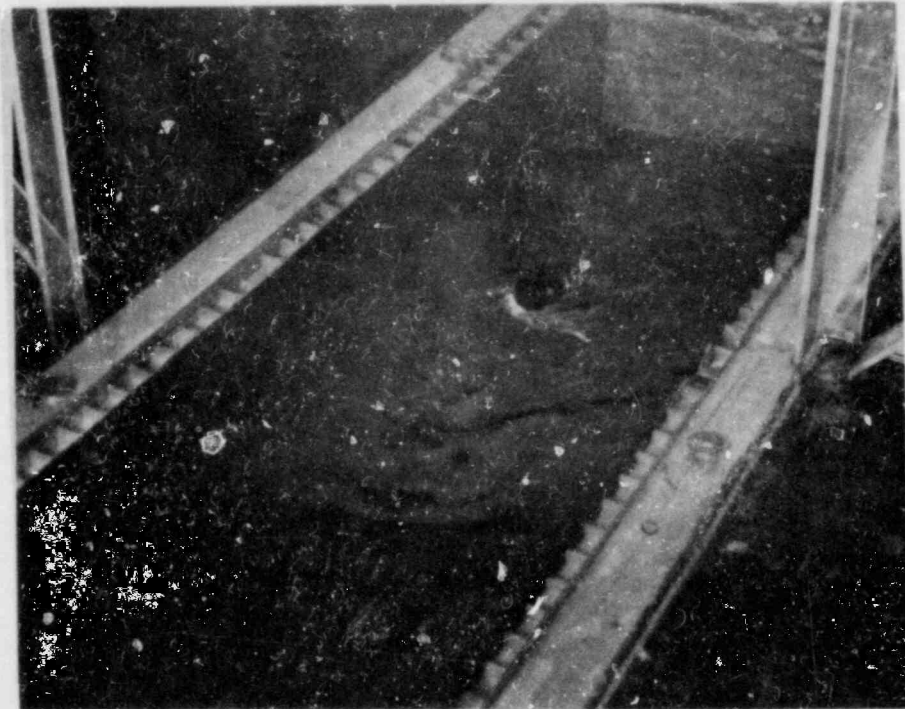
Photograph 3 Pressure Gradient Measurement Setup



Photograph 4 Vortimeter for Swirl Measurements



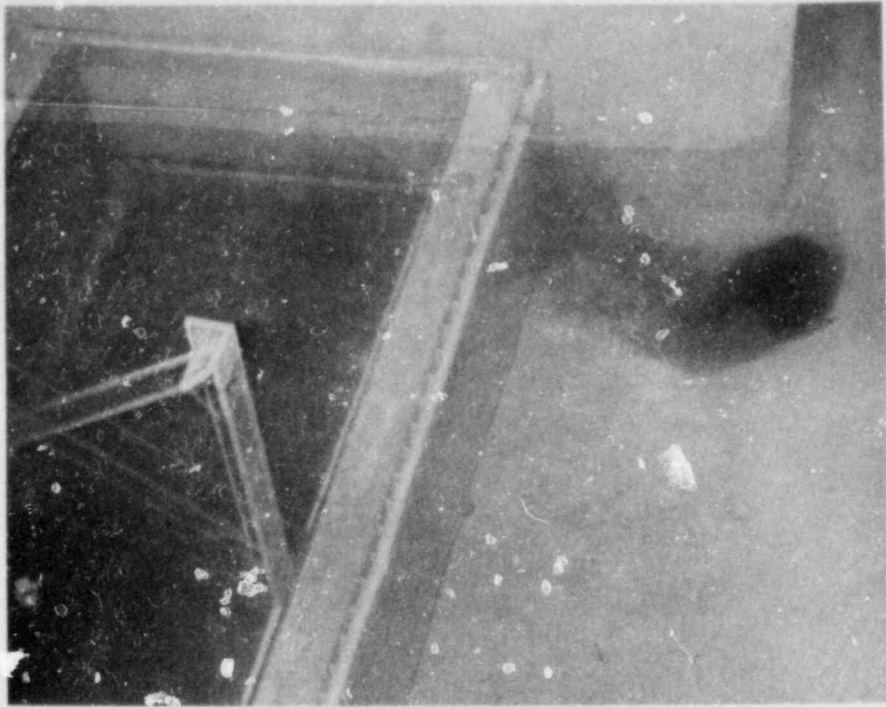
a. Scaled Velocity; $F_r = 1$



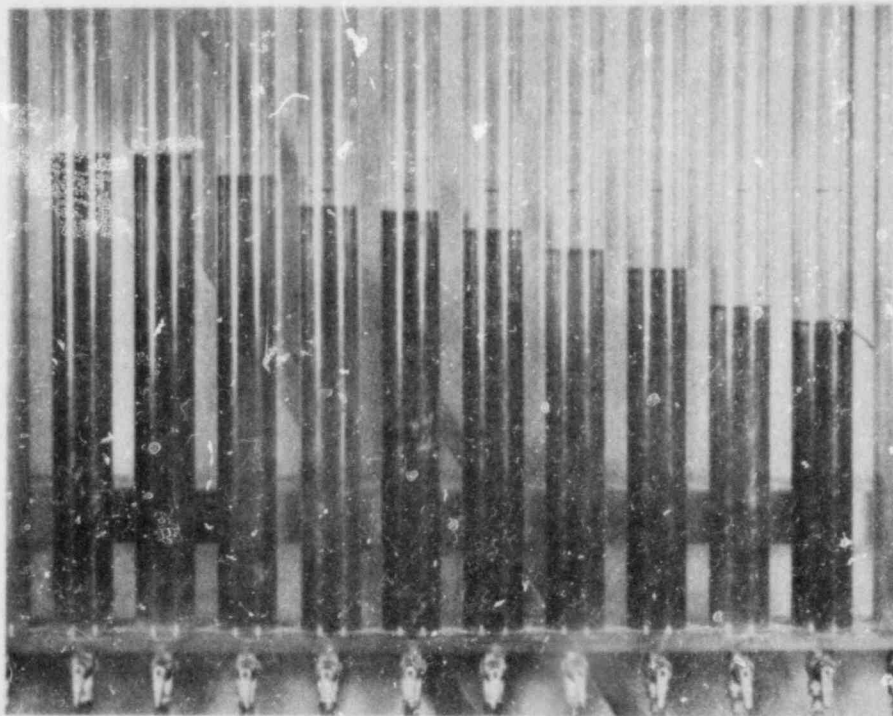
b. Prototype Velocity; $F_r = 2$

Photograph 5 Vortex Activity for Operating Case 8 at Minimum Water Level;
Screen Blockage Scheme 12

ARL



Photograph 6 Vortex Activity for Operating Case 8 at Maximum Water Level;
Screen Blockage Scheme 11; $F_r = 2$



Photograph 7 Typical Pressure Gradient; Pipe 2; Operating Case 8;
Blockage Scheme 12; $F_r = 2$

FIGURES

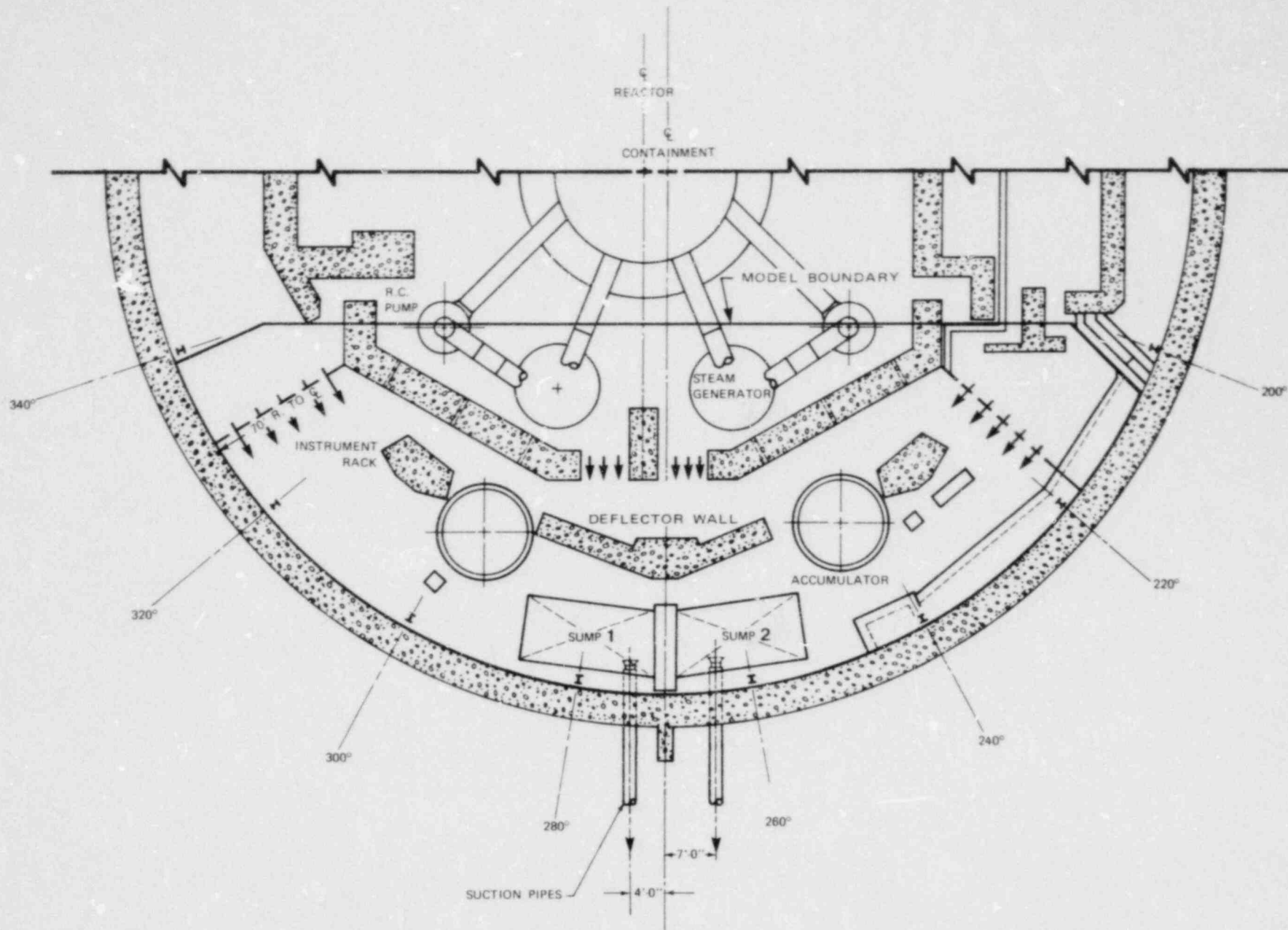
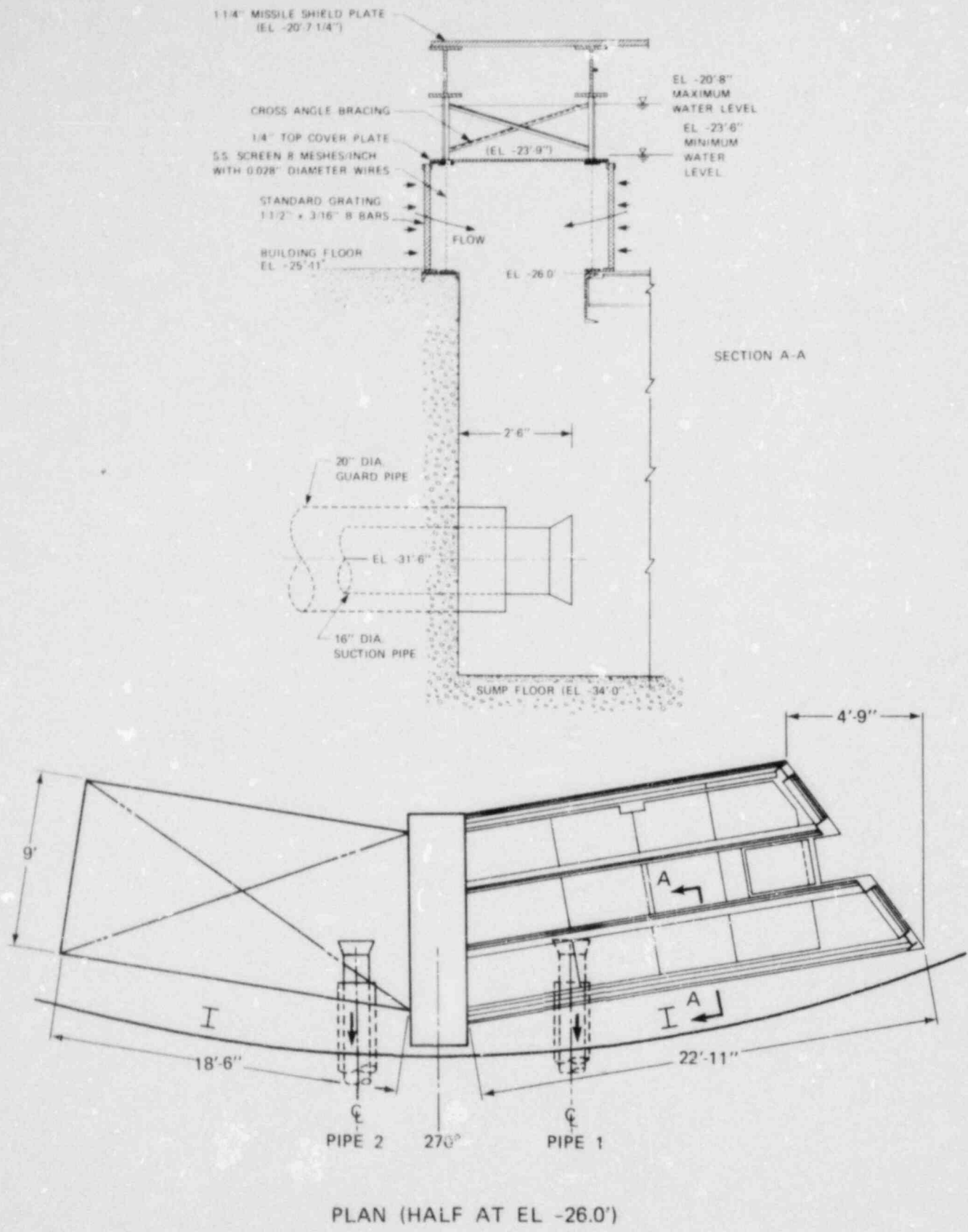
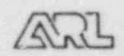


FIGURE 1 PARTIAL PLAN OF CONTAINMENT BUILDING



PLAN (HALF AT EL -26.0')

FIGURE 2 SUMP DETAILS



VORTEX
TYPE

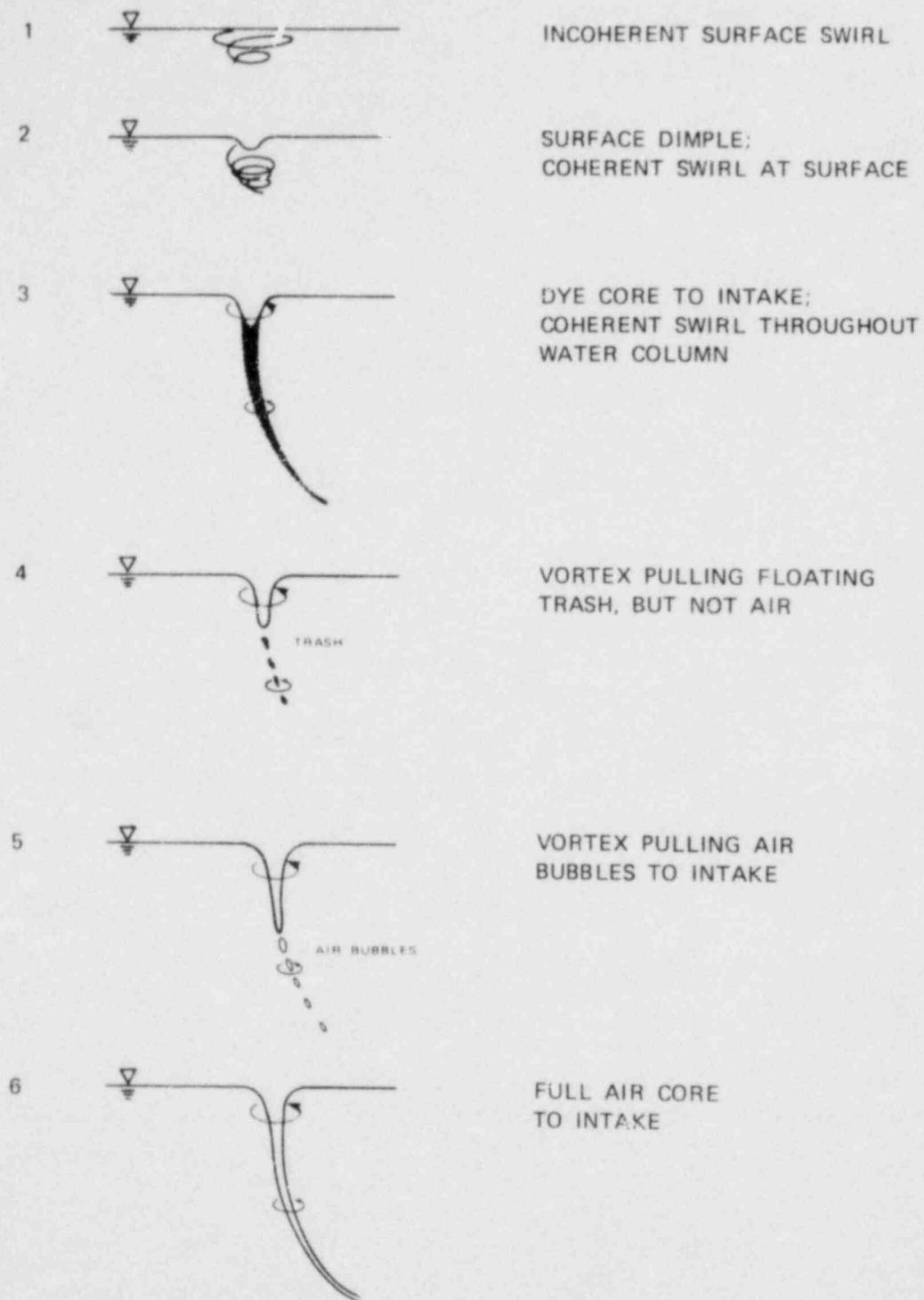


FIGURE 3 VORTEX STRENGTH SCALE
FOR INTAKE STUDY

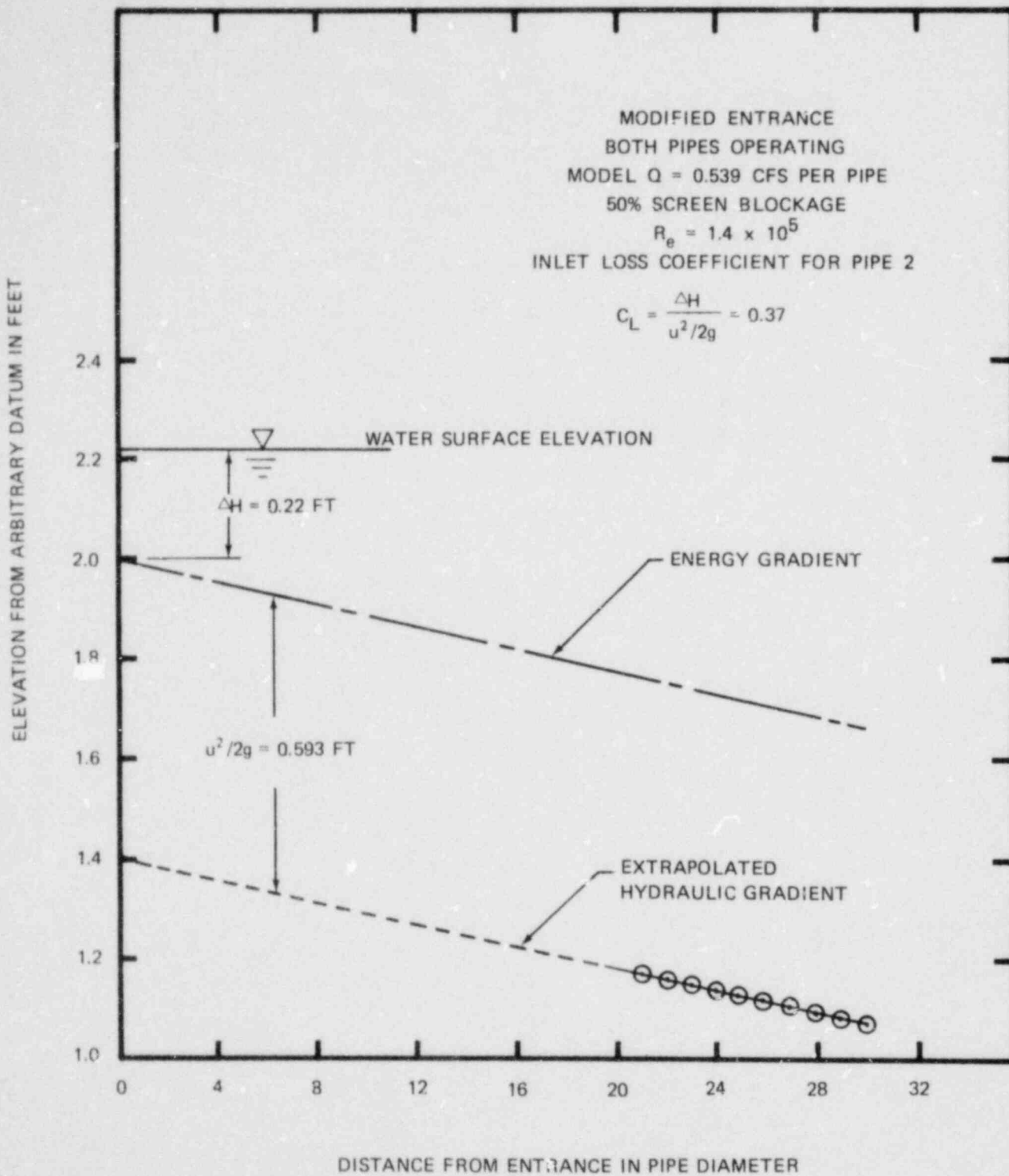
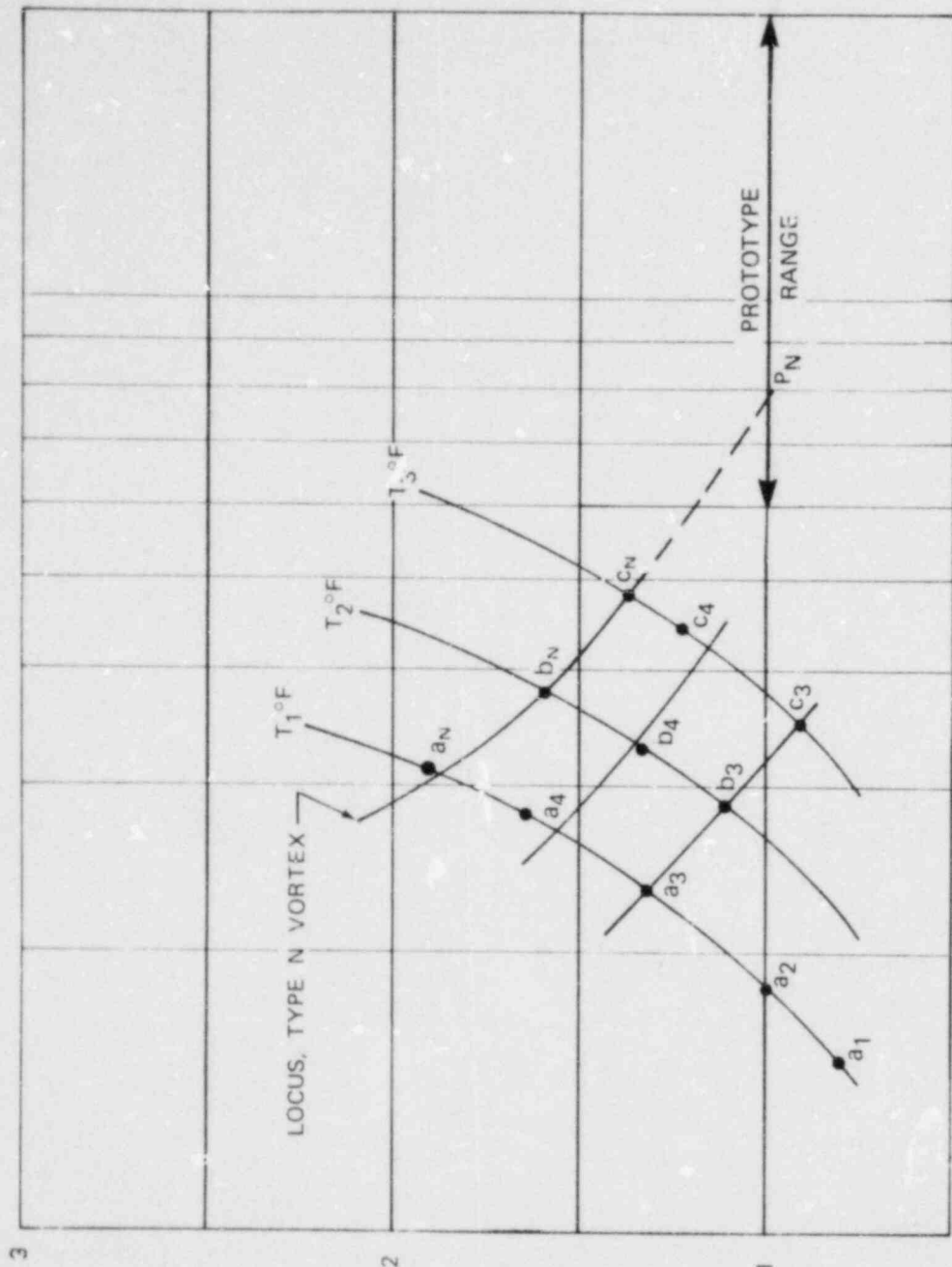


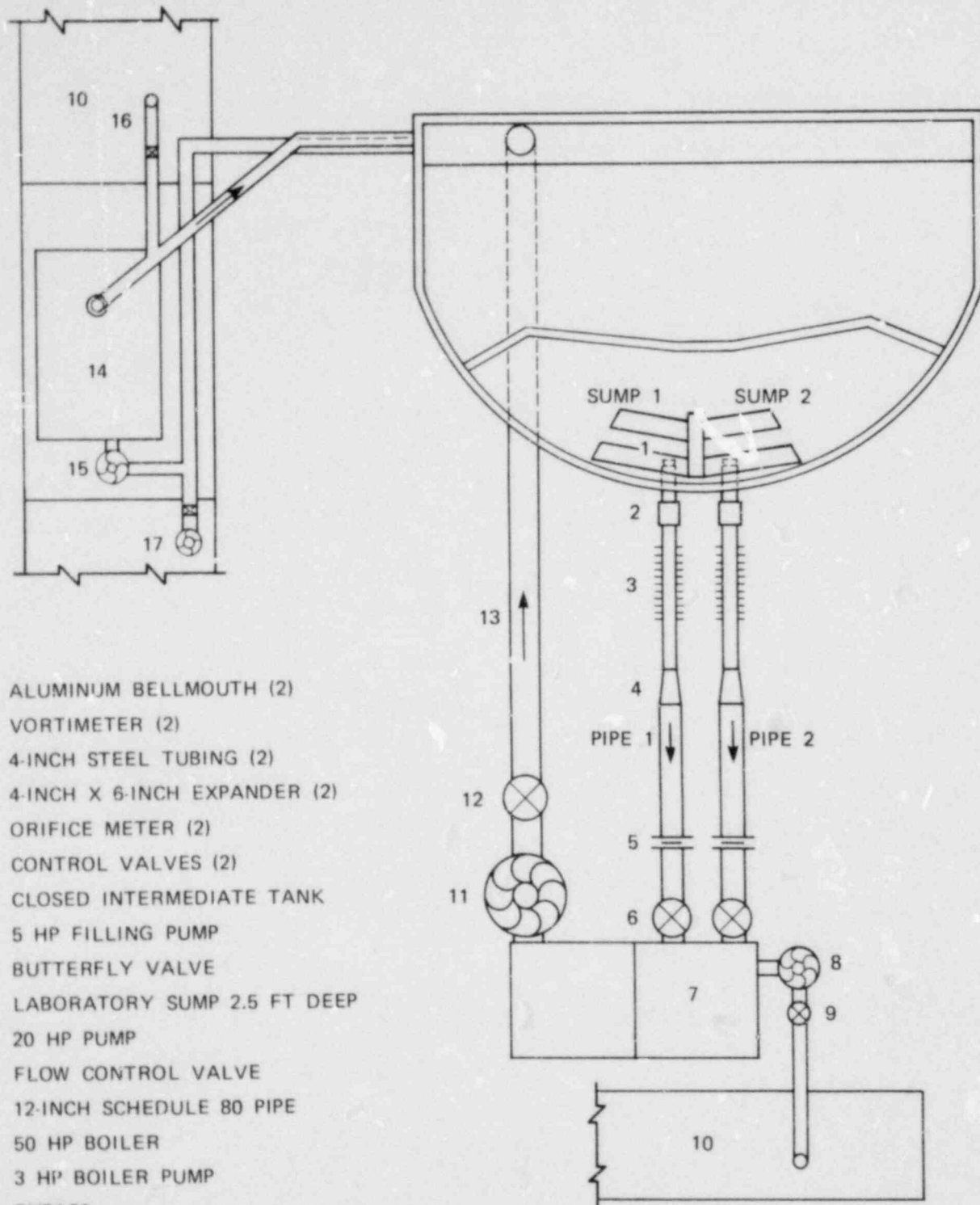
FIGURE 4 DERIVATION OF INLET LOSS COEFFICIENT



$$IF_r = \frac{IF_m}{IF_p}$$

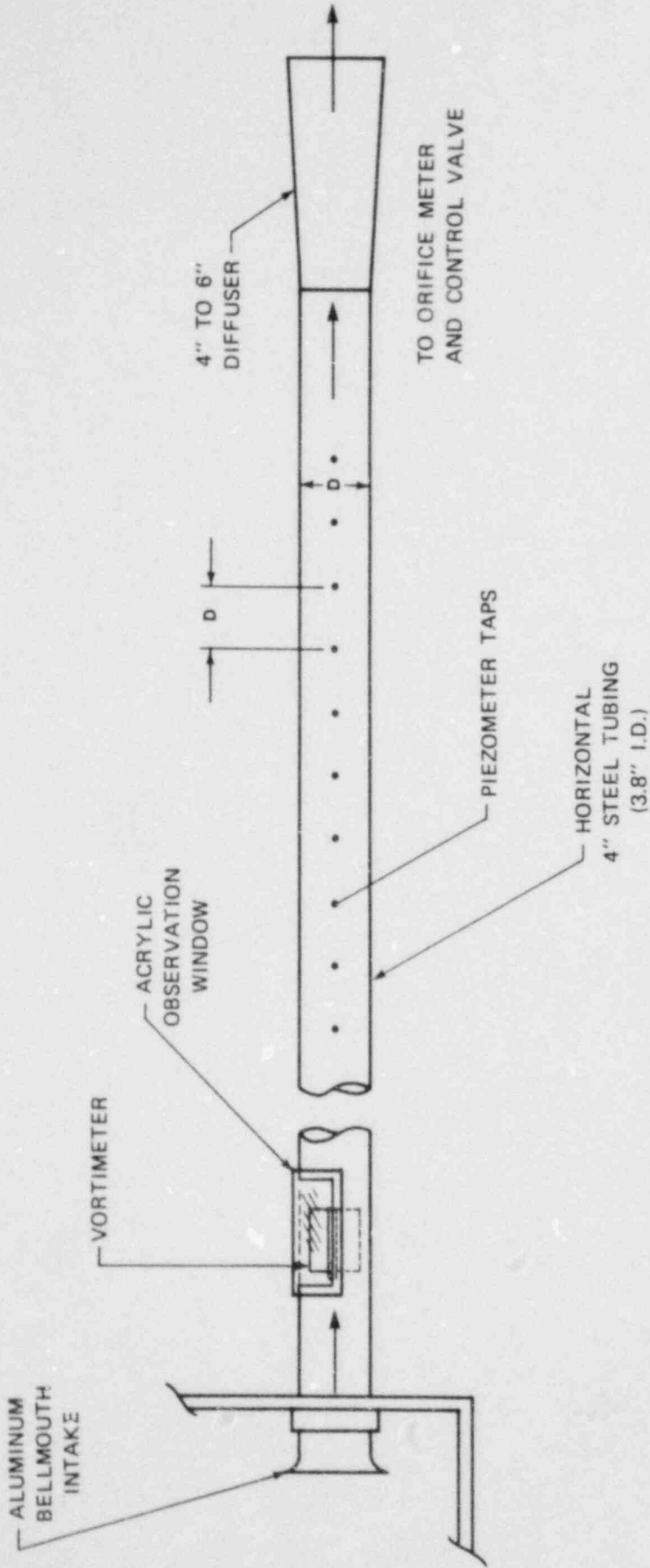
IR

FIGURE 5 DEPENDENCE OF VORTEX SEVERITY ON FROUDE AND REYNOLDS NUMBERS



1. ALUMINUM BELLMOUTH (2)
2. VORTIMETER (2)
3. 4-INCH STEEL TUBING (2)
4. 4-INCH X 6-INCH EXPANDER (2)
5. ORIFICE METER (2)
6. CONTROL VALVES (2)
7. CLOSED INTERMEDIATE TANK
8. 5 HP FILLING PUMP
9. BUTTERFLY VALVE
10. LABORATORY SUMP 2.5 FT DEEP
11. 20 HP PUMP
12. FLOW CONTROL VALVE
13. 12-INCH SCHEDULE 80 PIPE
14. 50 HP BOILER
15. 3 HP BOILER PUMP
16. BYPASS
17. DRAIN AND AUXILIARY FILLING PUMP

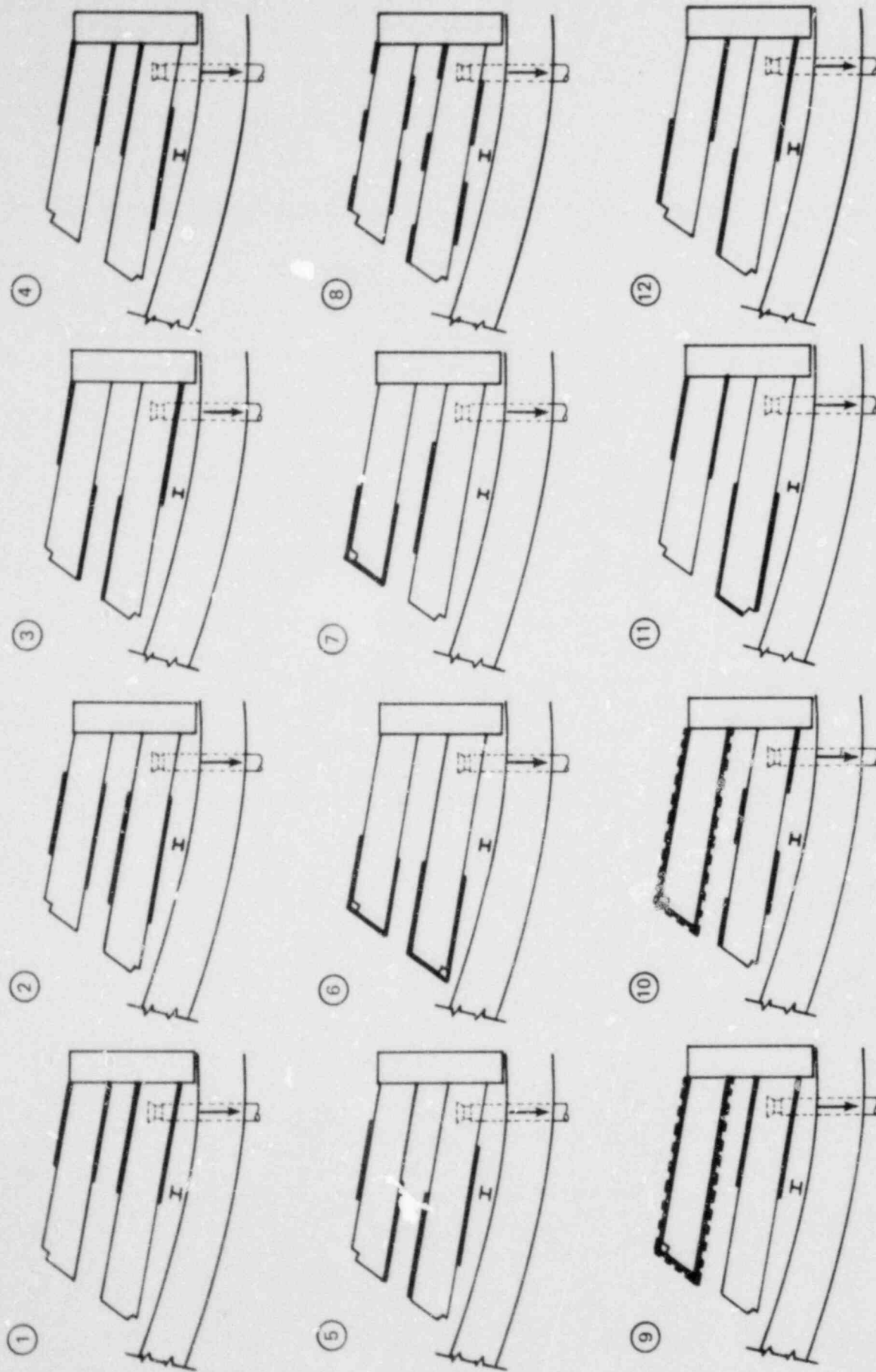
FIGURE 6 MODEL PIPE LAYOUT



NOTES:

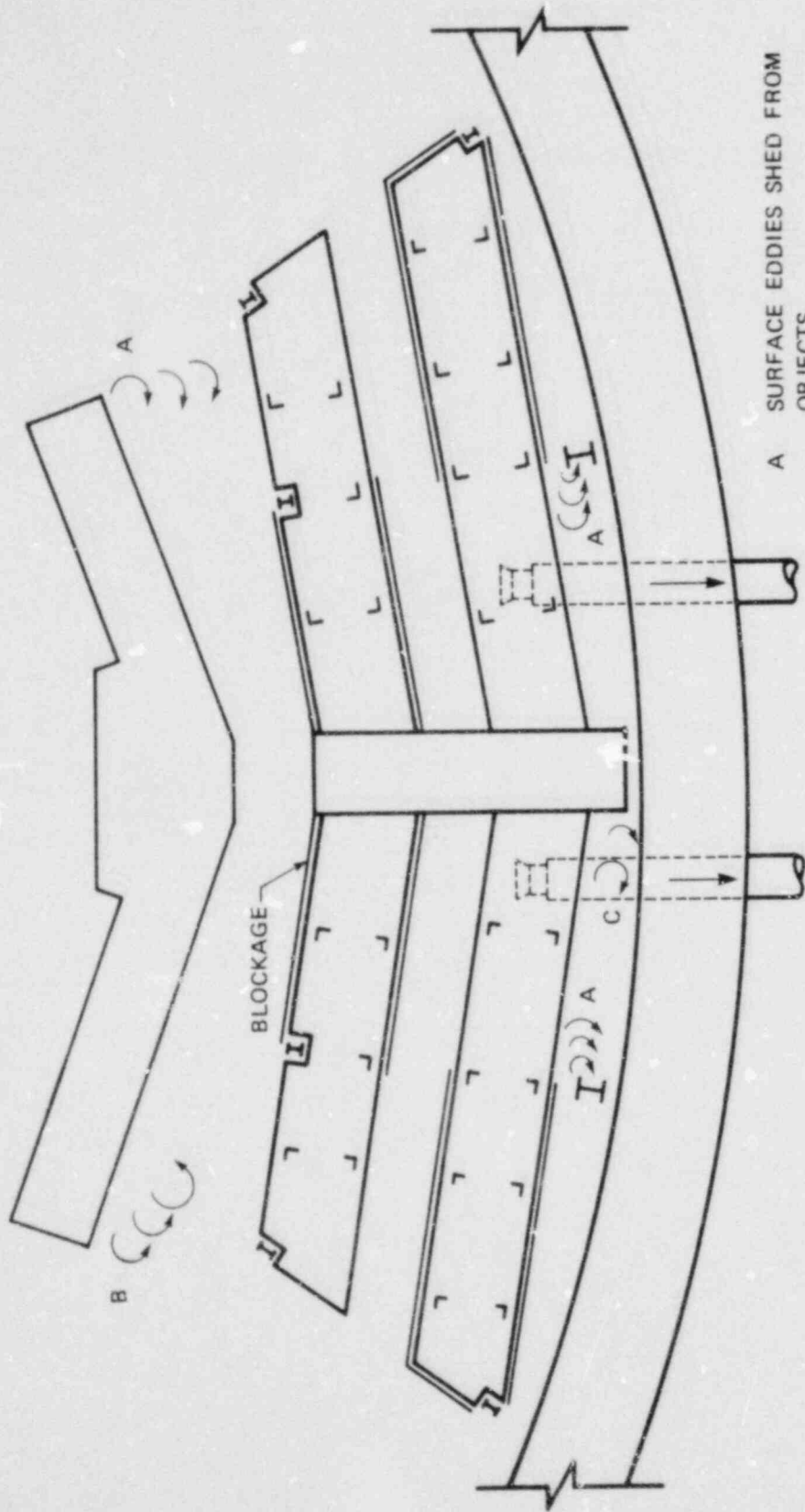
- IDENTICAL LAYOUT FOR BOTH SUMPS
- FIRST PRESSURE TAP LOCATED AT 21 DIAMETERS FROM BELL ENTRANCE
- MODEL PIPES ϕ 0.625 FT ABOVE SUMP FLOOR

FIGURE 7 SUCTION PIPE LAYOUT IN MODEL



NOTE: DOTTED LINE DENOTES 50% BOTTOM BLOCKAGE.

FIGURE 8 SCREEN BLOCKAGE SCHEMES TESTED



- A SURFACE EDDIES SHED FROM OBJECTS
- B SURFACE SWIRL AND DIMPLES DUE TO EDDIES; UNSTABLE
- C SURFACE DIMPLE; OCCASIONAL WEAK DYE CURVE; DISSIPATED ON PASSING THROUGH SCREEN

FIGURE 9a VORTEXING IN THE SUMP AREA; BOTH PIPES OPERATING; CASE 8;
 SCREEN BLOCKAGE SCHEME 11; MAXIMUM WATER LEVEL; $F_r = 2.0$

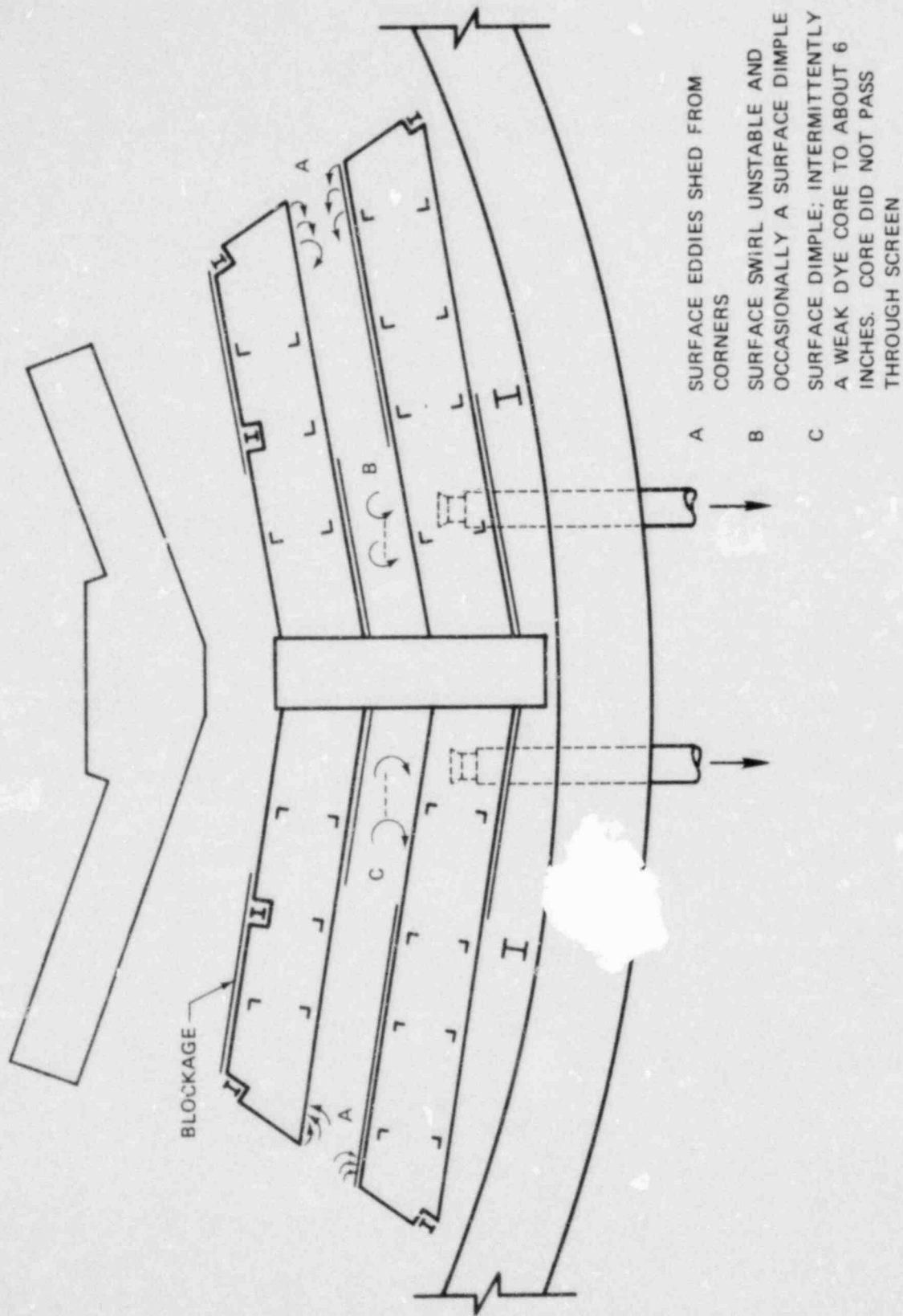


FIGURE 9b VORTEXING IN THE SUMP AREA; BOTH PIPES OPERATING; CASE 8;
 SCREEN BLOCKAGE SCHEME 12; MINIMUM WATER LEVEL; $F_r = 2.0$

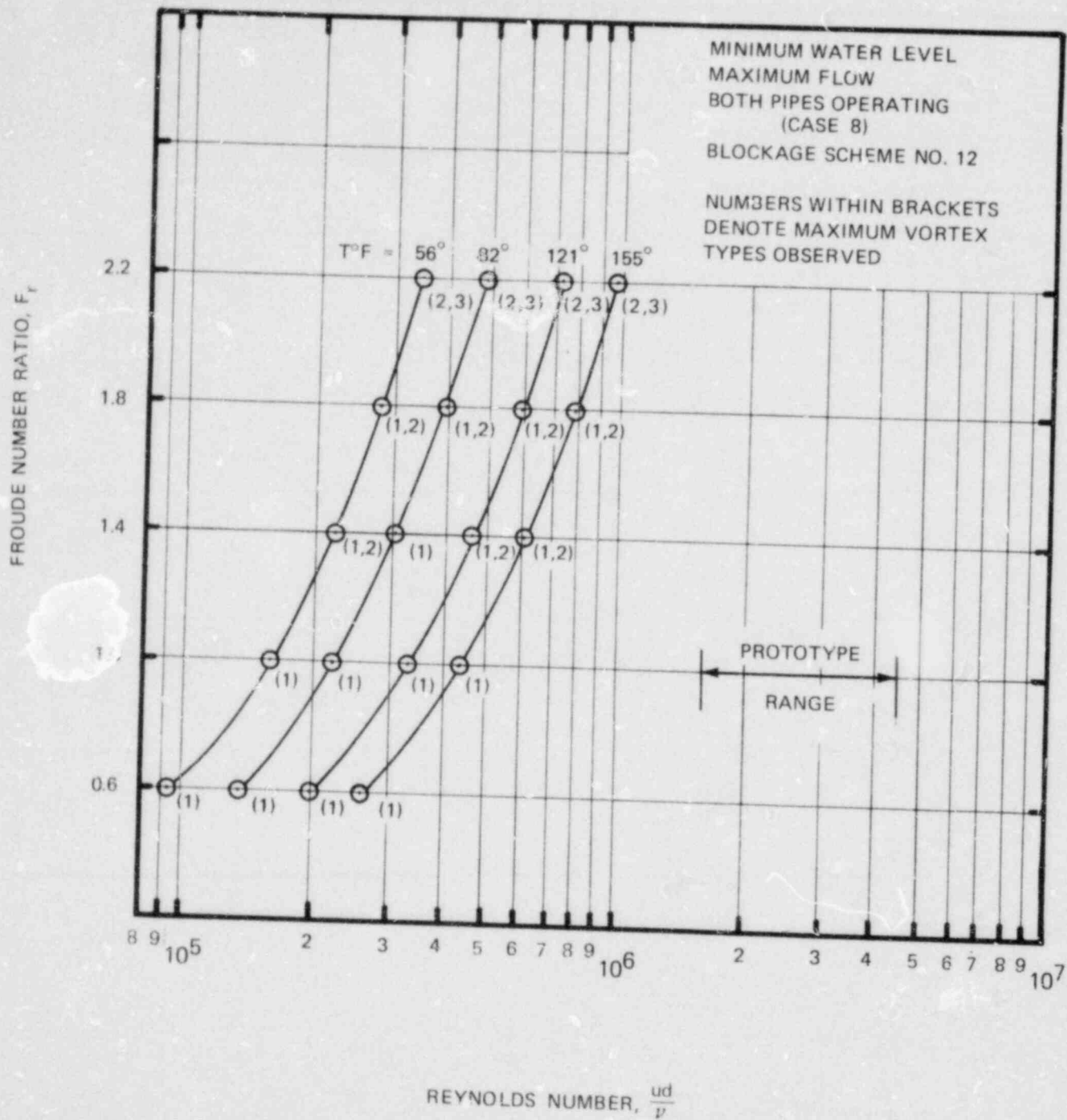


FIGURE 10 FROUDE NUMBER RATIO VERSUS REYNOLDS NUMBER SHOWING
 MAXIMUM OBSERVED VORTEX TYPES IN THE SUMP

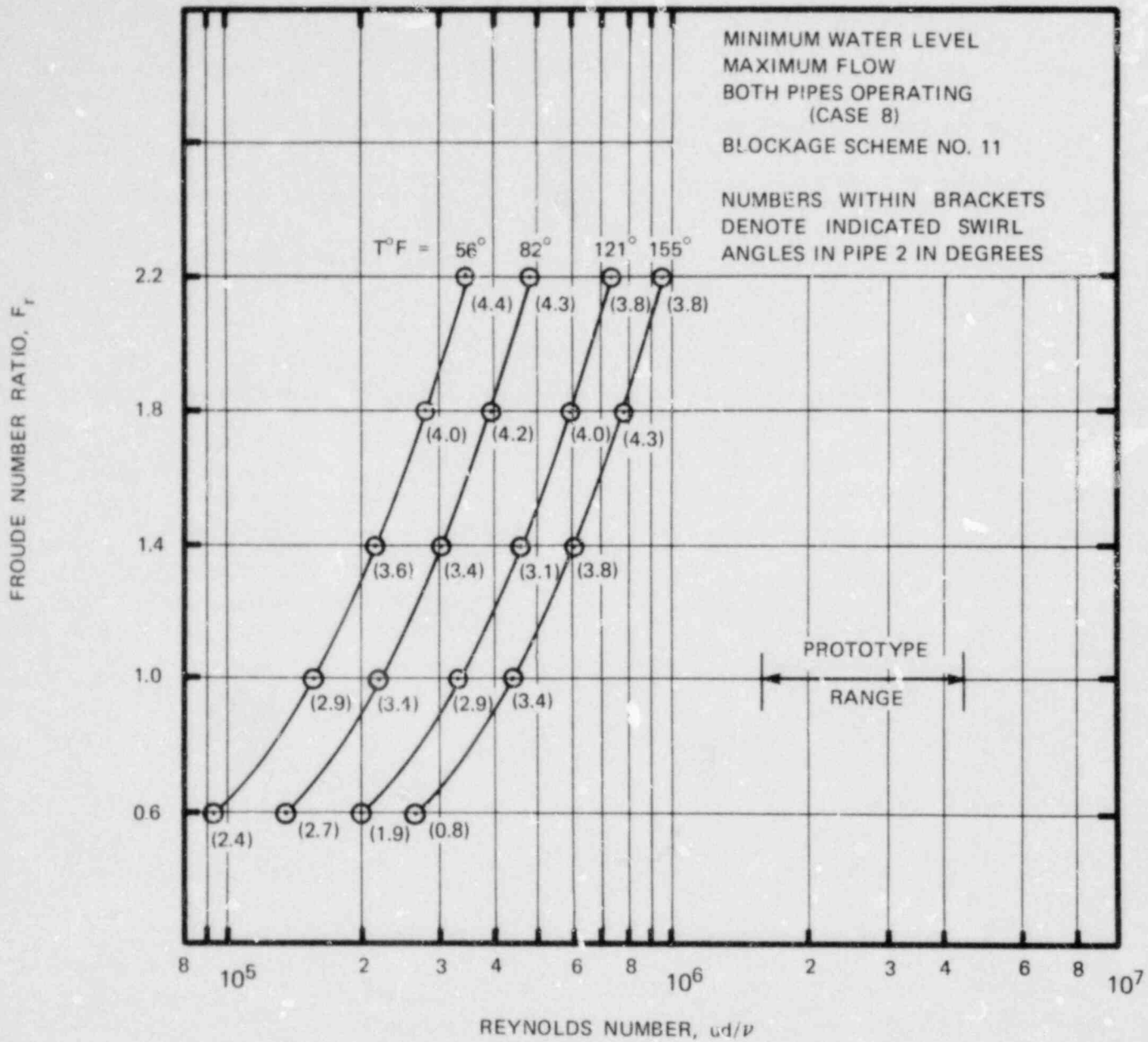
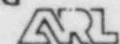


FIGURE 11 FROUDE NUMBER RATIO VERSUS REYNOLDS NUMBER SHOWING INDICATED SWIRL ANGLES IN PIPE 2



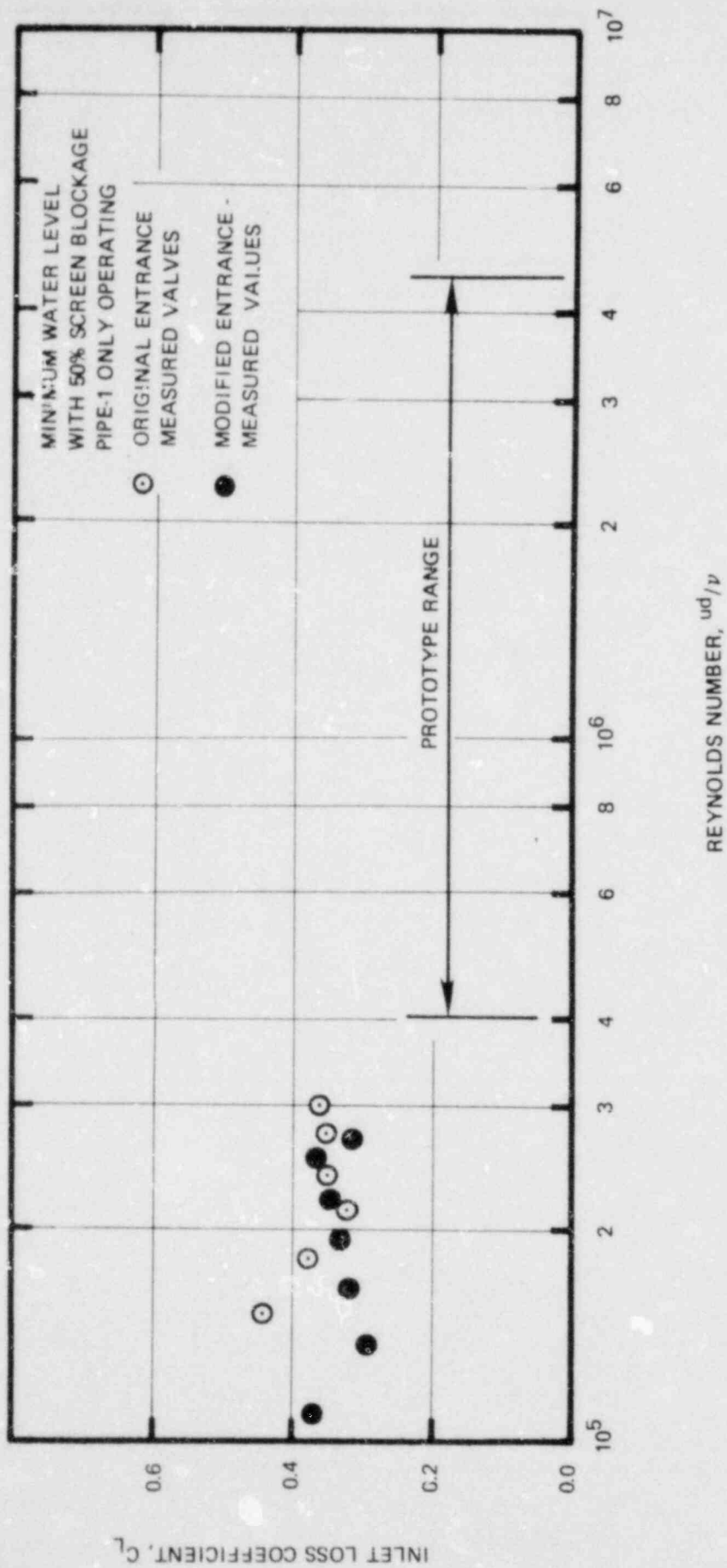


FIGURE 12 INLET LOSS COEFFICIENT FOR SINGLE PIPE OPERATION

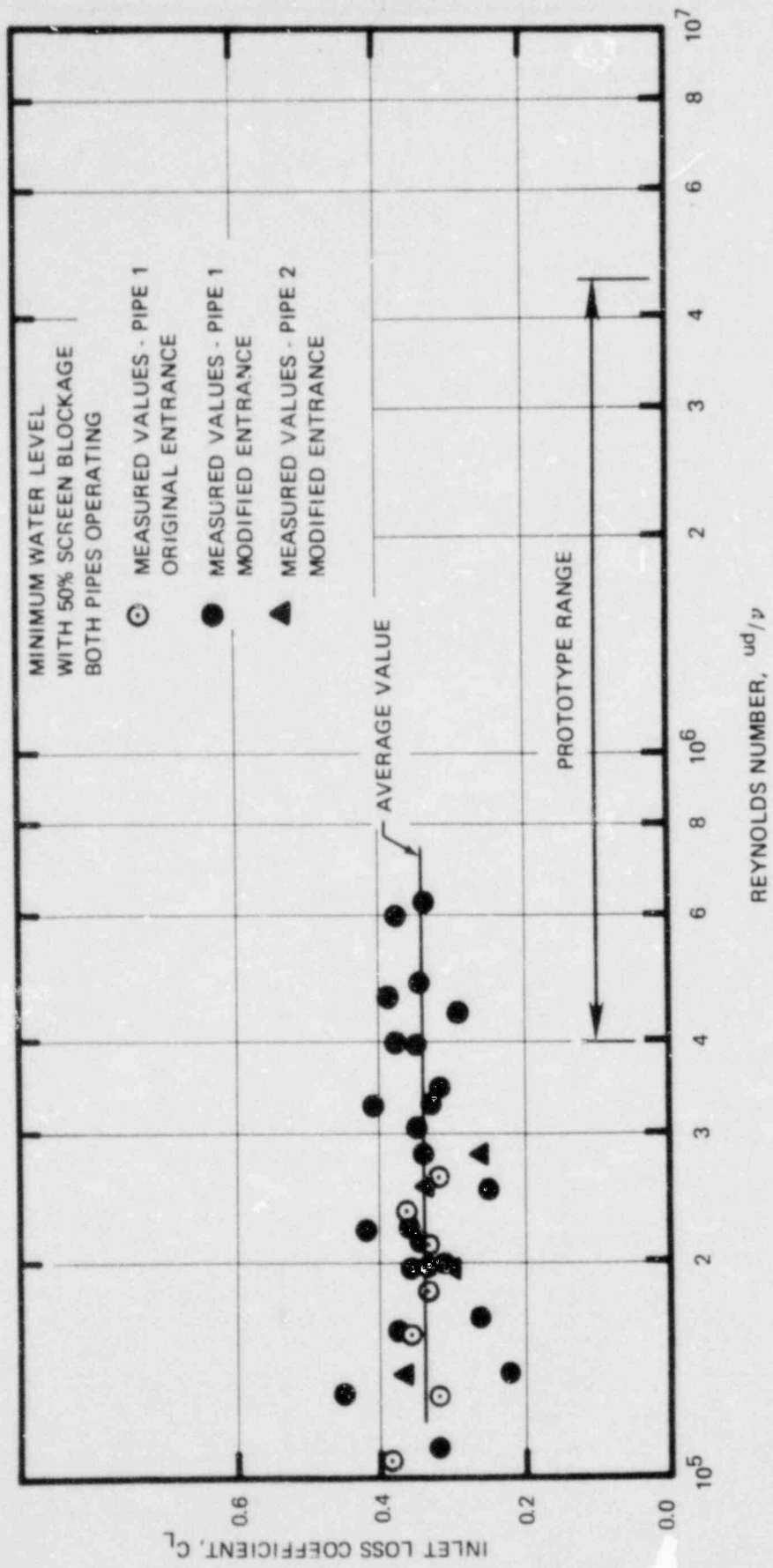


FIGURE 13 INLET LOSS COEFFICIENT FOR BOTH PIPES OPERATING

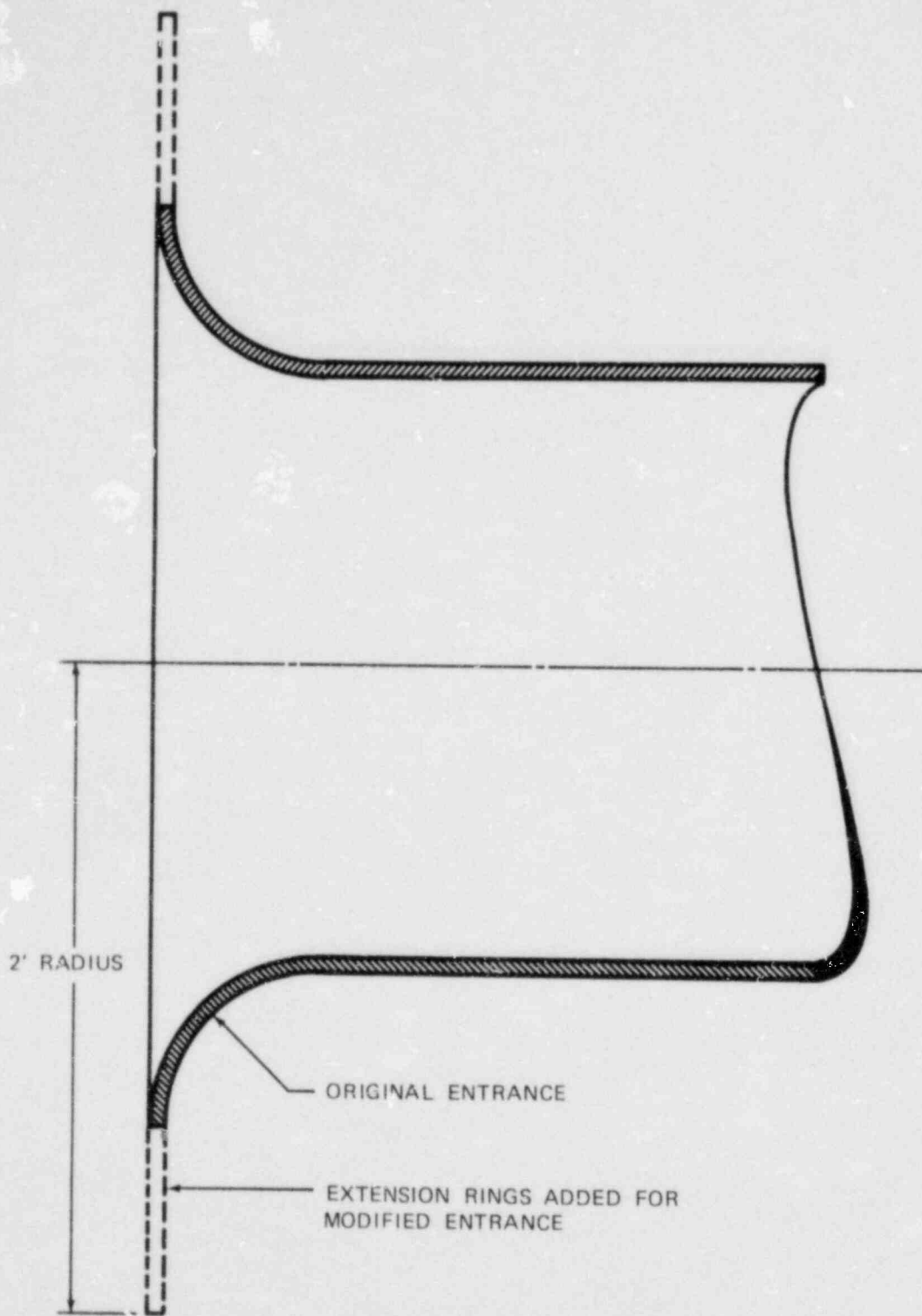


FIGURE 14 MODIFIED BELL ENTRANCE



WORCESTER
POLYTECHNIC
INSTITUTE

ALDEN RESEARCH LABORATORY
HOLDEN, MASSACHUSETTS 01520

ATTACHMENT NOT FILMED

ANO. 8112010642

NO. OF PAGES 450

DUPLICATE: ALREADY ENTERED INTO SYSTEM
UNDER ANO. _____

ILLEGIBLE: HARD COPY AT:

PDR

CF

OTHER _____